**Arab American University**

**Faculty of Graduate Studies**

# “MR spectroscopy (MRS) and MR spectroscopic imaging (MRSI) for the non-invasive evaluation of glioblastoma multiform (GBM) tumors “


By

Yasser Mohammad Mansour

Supervisor:

Dr. Abed Al Naser Assi


This thesis is submitted in partial fulfillment of the requirements for the Master's degree in Computed Tomography and Magnetic Resonance Imaging

Oct-2023

## Thesis Approval

# “MR spectroscopy (MRS) and MR spectroscopic imaging (MRSI) for the non-invasive evaluation of glioblastoma multiform (GBM) tumors “

Prepared by: Yasser Mohammad Ibrahim Mansour

Registration No: 202113120

Supervisor: Dr. Abed Al Naser Assi

Co-Supervisor:

This thesis was defended successfully on 25/10/2023 and approved by:

| Committee members | signature |
| --- | --- |
| 1. Dr. Mohammad Aljamal |  |
| 2. Dr. Ala Habboub | 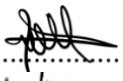 |
| 3. Dr. Abed Al Naser Assi | 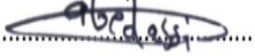 |

Ramallah – Palestine
1445 / 2023

## Declaration

I certify that this thesis submitted for the degree of the master is the result of my research, except where otherwise acknowledged, and that the thesis has not been submitted for a higher degree to any other university or institution.

Signed: 

Yasser Mohammad Ibrahim Mansour

Student ID: 202113120

Date: 25.10.2023

## Dedication

I dedicate this project to God Almighty my creator.

My strong pillar is my source of inspiration, wisdom, knowledge, and understanding.

My Family

They have been the source of my strength throughout this program.

My lovely wife

For her endless patience and support and my source of encouragement

My sweet and adorable children

My friends and everyone who helped me and believed in me.

To martyrs and detainees

To my people

## Acknowledgment

I would want to begin by thanking Allah, my Creator, for the excellence of His grace and for allowing me to finish this effort.

To complete this task, I must acknowledge and extend my sincere gratitude to my supervisor, Dr. Abed Al Naser Assi. His help, encouragement, and counsel got me through every phase of writing my study. Additionally, I would like to thank Dr. Mohammad Zohd for his work on this study. Additionally, I would like to express my gratitude to my coworkers who work as medical imaging techs at government hospitals for their unending assistance and support in completing this study.

Additionally, I want to express my gratitude and special thanks to my mother, who is my inspiration, and the rest of my family for their unwavering support.

My sincere appreciation to my wife and kids who have put up with years of missing leisure time and the added workload due to my absence.

My sincere appreciation is extended to my closest friends and coworkers for their assistance and motivation.

Finally, I'd like to thank everyone at the AAUP and the Computed Tomography and Magnetic Resonance Imaging program for letting me conduct this study. And I must express my gratitude to the research team at the hospital and the Palestinian Ministry of Health.

I want to thank everyone who helped. Thank you to everyone who assisted and encouraged me in completing this research.

## Table of Contents

# List of Table

# List of Figures

## List of Abbreviations

AAUP: Arab American University.

GBM: Glioblastoma Multiform.

MRI: Magnetic Resonance Imaging.

1HMRS: Proton Magnetic Resonance Spectroscopy.

MRS: Magnetic Resonance Spectroscopy.

MRSI: Magnetic Resonance Spectroscopy Imaging.

BM: Brain Metastasis.

NAA: N-Acetyl Aspartate.

Pcho: Phosphocholine.

Cr: Creatine.

PMC: Palestine Medical Complex.

BBB: Blood-Brain Barrier.

CNS: Central Nervous System.

PFS: Progression-Free Survival.

STEAM: Stimulated Echo Acquisition Mode.

PRESS: Point Resolved Spectroscopy.

SPECIAL: Spin-Echo Full-Intensity Acquired Localized Spectroscopy.

CHESS: Chemical Shift Selective Suppression.

TE: Time Echo.

PPM: Part Per Million.

T: Tesla.

GE: General Electric

# Abstract


## Introduction

Glioblastoma multiforme (GBM) is the most common and frequent tumor of the adult population's central nervous system, making up 40% of all brain tumor types and 15% to 20% of high-grade tumors. A critical public health issue, GBM is a rare tumor with a global incidence of less than 10 per 100,000 persons and a survival rate of 14–15 months after diagnosis. In all age categories, it accounts for 50% of all gliomas.

A non-invasive imaging method called magnetic resonance spectroscopy (MRS) is used to examine metabolic alterations in brain malignancies. The current work used MRS multivoxel to investigate significant metabolites in GBM tumors. Since its first report in the 1980s, the human brain's magnetic resonance spectroscopy (MRS) has advanced quickly. Because it can be performed without requiring hardware modification on most MRI machines, unlike MRS of other nuclei, proton MRS became more and more popular in the 1990s because of its improved spatial localization and water suppression techniques as well as because of its increased sensitivity and convenience. An MRI scanner is utilized for the evaluation.

## Purpose of the study

The purpose of this study is to evaluate and diagnose glioblastoma multiforme (GBM) using a non-invasive imaging method called magnetic resonance spectroscopy (MRS) to ability replace the biopsy to save the patient from having to undergo biopsy surgery and its associated hazard.

## Methods of the study

The study was a quantitative, cross-sectional, interventional study to evaluate the glioblastoma multiform using MR Spectroscopy and the effectiveness of the MRS to dispense with a biopsy in the MRI department work practice of Palestinian governmental hospitals, especially in Palestine Medical Complex (PMC) MRI department.

From October 2022 to June 2023, data on 7 patients with GBM (2 patients new and 5 patients with tumor resection), 1 patient with metastatic disease, 1 patient with meningioma, and 1 patient with oligodendroglioma were gathered for this study. Utilizing a magnetic field strength of 1.5 Tesla and employing GE multivoxel Magnetic Resonance Spectroscopy (MRS), we conducted the Point-Resolved Spectroscopy (PRESS) procedure with an Echo Time (TE) of 144 ms and a Repetition Time (TR) of 1570 ms to acquire the data. Statistical analysis was subsequently applied to the extracted metabolites, including Pcho, NAA, Cr, Pcho/Cr ratio, Pcho/NAA ratio, NAA/Cho ratio, NAA/Cr ratio, and Cr/NAA ratio, to meticulously examine the spectroscopic data.

## Results

For the total numbers of voxels of GBM, whether normal or tumoral, the level of metabolic ratio values of NAA/Cr, NAA/Pcho, Pcho /Cr, Pcho /NAA, and Cho concentration, were (1.24 ± 0.68, 0.90 ± 0.54, 1.81 ± 1.11,1.91 ± 2.08, 66999.17 ± 51226.74) respectively for the tumoral voxel and (2.34 ± 1.39, 1.67 ± 0.56, 1.49 ± 0.95, 0. 69 ± 0.34, 62585.15 ± 37676.36) respectively for normal

voxel, the ratio of the tumoral voxel were significantly higher than the normal ratio, and the concentration of Cho higher than the normal voxel.

## Conclusion

The results of the current study showed that the most important and useful criteria for identifying tumoral and normal voxels in patients with glioblastoma who have 1HMRS are the NAA, Pcho/Cr, Cr/NAA, and Pcho/NAA ratios. However, due to the low sensitivity and specificity of the results, we cannot replace the diagnosis obtained through biopsy with MRS. Nevertheless, we can rely on MRS as a secondary diagnostic tool.

The most accurate diagnostic test was Pcho/NAA, with a sensitivity of 83.3% and a specificity of 28.8%. Cr/NAA was the second efficient test (sensitivity: 78.2%, specificity: 35.6%). The Pcho/Crea Ratio was the third helpful test (sensitivity: 61.5%; specificity: 40.7%).

# CHAPTER ONE

# INTRODUCTION

## 1.1. Background

Glioblastoma multiform (GBM) is the most prevalent and dangerous brain tumor, which accounts for 40% of all brain tumors and 15% to 20% of high-grade tumors. More than half of the 2607 people in the United States with malignant brain tumors in 2017 had GBMs. The reported 5-year survival rate with therapy is 9.8%, and the median survival time for GBM patients undergoing treatment is 14.6 months, compared to 6.9 months for those who are not receiving treatment (Mansoory *et al.*, 2020). According to epidemiological data, 2-3 GBM instances are reported for every 100,000 adults annually in Europe and North America (Urbanska *et al.*, 2014). The incidence rate for males versus women is 1.26:1 (Urbanska *et al.*, 2014). There have also been reports of GBM in neonates and infants. According to estimates, this tumor affects between 1.1 and 3.6 infants per 100,000, with 3.3 male children diagnosed with glioblastoma for every female kid. No anatomical distinctions exist between GBM in children and adults (Urbanska *et al.*, 2014). A critical public health issue, GBM is a rare tumor with a global incidence of less than 10 per 100,000 persons and a survival rate of 14–15 months after diagnosis. In all age categories, it accounts for 50% of all gliomas (Hanif *et al.*, 2017). Glioblastoma (GBM) is the most prevalent primary malignant brain tumor. The current course of treatment entails doing the maximum safe resection, then radiation with concurrent and adjuvant temozolomide. However, the survival rates at 2, 3, and 5 years are just 27%, 16%, and 9.8%, respectively. The inadequate local control following treatment is one of the key causes of this poor prognosis. Within 2 cm of the initial tumor, up to

77% of GBM recurrences occur, and 72% of cases occur in the radiation therapy zone (Yan *et al.*, 2019).

An effective technique for diagnosing GBM tumors that allows for anatomical visualization of the brain tumor is magnetic resonance imaging (MRI). In MRI imaging, GBMs are shown as ring-enhancing lesions. This pattern, meanwhile, is not specific to GBM and can also be seen in conditions including metastasis, abscess, and multiple sclerosis. The spatial spread of cancerous cells in the brain cannot be seen using MR methods, despite the significant contrast of soft tissue in MRI images for the site of the GBM tumor. Any sort of treatment, including surgery, chemotherapy, or radiation, requires the capacity to discern between healthy and tumorous tissues (Arcalis *et al.*, 2011).

The precise geographical location of the tumor must be determined, which requires an in-depth understanding of brain tissue. Neurological disorders have an impact on the concentration of metabolites in brain tissue, such as phosphocholine (Pcho), creatine (Cr), and N-acetyl aspartate (NAA), as well as concentration ratios like NAA/Cr and Pcho/Cr. The metabolic profile of brain tissue may be ascertained via non-invasive proton magnetic resonance spectroscopy (1HMRS), including the concentration and distribution of metabolites.) Magnetic Resonance Spectroscopy (MRS) has been used to assess several forms of brain tumors and is demonstrated as a clinical tumor assessment component. According to research by Einstein et al. patients who get stereotactic radiosurgery outlive conventional therapies for patients with (Pcho/NAA) > 1.1 (Einstein *et al.*, 2012). In voxels before radiotherapy, a concentration ratio of (Lac/NAA)>=0.4 may be used to predict the tumor's recurrence (Deviers *et al.*, 2014).

Important brain metabolites including NAA, Pcho, Cr, glutamic acid (Glu), and glutamine (Gln) were initially introduced by Haaga et al. The NAA metabolite, in particular, is important for neurological illnesses, especially brain tumors. Additionally, they found that the NAA/Cr and Pcho/Cr ratios in GBM tumors changed in a manner that was opposite to that of healthy brain tissue (Mansoory *et al.*, 2020). According to Parra et al. the distribution of metabolites like NAA and Pcho in healthy and tumoral voxels varied significantly. Tumoral voxels showed greater Pcho concentrations and lower NAA concentrations than healthy voxels (Parra *et al.*, 2014).

By analyzing MRS data, Crain et al. found that five ratios—Pcho/Cr, Cr/Pcho, NAA/Pcho, and Pcho/NAA—help to discriminate between healthy and tumoral voxels in GBM (Crain *et al.*, 2017). The concentration of metabolites in MRS signals has been quantified using a variety of approaches, however, the quantifications are still subject to large fluctuations and inaccuracies (Dezfouli *et al.*, 2017). Recent research has demonstrated that by utilizing MRS multivoxel data, unknown metabolites or ratios may need to be assessed for GBM tumors. These ratios and their metabolites were studied (Mansoory *et al.*, 2020).

### 1.2. Problem statement

The primary diagnostic technique for GBM is magnetic resonance imaging. At the time of diagnosis, the tumor is usually about 4 cm in diameter (Urbanska *et al.*, 2014). The resected intraoperative tumor or any of its components must be examined histologically using conventional histological, cytological, and histochemical techniques to provide a conclusive diagnosis

(Urbanska *et al.*, 2014). A procedure known as a small needle biopsy is used when neurosurgical removal of the tumor is not an option (Urbanska *et al.*, 2014). The biopsy sampling procedure that can be used in approaching the diagnosis of GBM is an invasive technique and it has several drawbacks because the patient will be under anesthesia for sampling which necessitates patient safety and absence of respiratory diseases among others. In addition, it requires some lengthy preparations that may take days or even months. As it is known, GBM disease is a rapidly spreading disease, so the use of a biopsy in the diagnostic process will help to quickly spread this dangerous disease to the rest of the body. Hence, in this research, we will employ Magnetic Resonance Spectroscopy (MRS), a non-invasive technique known for its safety, speed, and high diagnostic accuracy, eliminating the need for surgical intervention.

## 1.3. Aims and Objectives

### 1.3.1. Aims

The purpose of this study is to evaluate and diagnose glioblastoma multiforme (GBM) using a non-invasive imaging method called magnetic resonance spectroscopy (MRS) to ability replace the biopsy to save the patient from having to undergo biopsy surgery. And spare the patient its associated hazards.

### 1.3.2. Objectives

To validate the effectiveness of magnetic resonance spectroscopy (MRS) in diagnosing glioblastoma, a coordinated effort will be established between the neurosurgery and oncology departments at the Palestine Medical Complex (PMC). Patients suspected of having brain tumors

will first undergo conventional magnetic resonance imaging (MRI) scans. If glioblastoma is suspected, MR spectroscopic examinations will then be conducted.

The research will involve the analysis and study of data from 7 patients with glioblastoma (2 patients new and 5 patients with tumor resection), encompassing both high-grade and low-grade tumors, as well as neoplastic and non-neoplastic GBM tumors. This research will be conducted over a span of ten months and will focus on patients in the West Bank region.

For this study, a GE Optima 360 1.5 Tesla MRI machine equipped with a 16-channel head coil will be utilized. The obtained data will undergo careful examination and review by a radiologist.

Following the imaging procedures, patients will receive follow-up care from neurologists to monitor their diagnosis progress and obtain biopsy results.

To assess the precision and effectiveness of MR Spectroscopy, the results obtained from biopsies will be compared with the MR Spectroscopy findings.

### 1.4. Hypotheses of research

It is hypothesized that GBM diagnosis depends on the MR spectroscopy will remove the danger of risk obtaining the biopsy and the diagnosis becomes rabidly and the treatment process will begin as soon as possible.

## 1.5. Questions of research

1-How MRS can help diagnose GBM early?

2- How to achieve MRS to diagnose GBM and become a dependable Test?

3- Can other malignant tumors in the brain can be detected with the MRS test?

## 1.6. Outline

Upon perusing the remainder of this thesis, you will encounter the subsequent chapters presented sequentially: -

1- Chapter (2): theory and a literature review with subtopics.

2- Chapter (3): methodology of the study and our research design.

3- Chapter 4: the result of the research.

4- Chapter (5): the discussion & and conclusion of the results.

# CHAPTER TWO

# LITERATURE REVIEW

## 2.1. Introduction:

This study was concerned with the diagnosis of GBM tumors by using MRS imaging in the West Bank. The chapter includes a literature review and theory of GBM disease and MRS techniques. For this study, the theory involved comprehensive research with keywords: GBM disease and its definition, Current methods of diagnosing GBM tumor, the difference between GBM tumor and other tumors, treatment of GBM tumor, we will discuss the MRS technique, the literature review involved comprehensive research with keywords: the effectiveness of the MRS technique in diagnosing GBM tumor.

Published studies in PubMed, Google Scholar, and textbooks were investigated in this study as a search strategy.

## 2.2. THEORY

### 2.2.1. Glioblastoma Multiform (GBM)

#### 2.2.1.1. Definition

In the latter half of the nineteenth century, Cushing coined the name "glioblastoma multiforme" (GBM), and the first operation on a patient with this kind of tumor was carried out in Vienna in 1904 (Urbanska *et al.*, 2014). The most malignant and common brain tumor, glioblastoma

multiforme (GBM), accounts for 40% of all brain tumor types and 15 to 20% of high-grade tumors (Tome-Garcia *et al.*, 2017).

GBMs were present in 2607 malignant brain tumor patients in the United States in 2017. Patients with GBM who are undergoing therapy and those who are not given therapy are both experiencing median survival times of 14.6 months and 6.9 months, respectively. 9.8% is the reported 5-year survival percentage upon receiving therapy (Mansoory *et al.*, 2020).

A primary brain tumor known as glioblastoma multiforme is made up of a variety of tumors that are geographically and phenotypically diverse (Ohgaki and Kleihues, 2013). Ninety percent of glioblastoma multiforme cases arise from normal glial cells in a multistep tumorigenic process (primary glioblastoma). The other 10% of gliomas are secondary neoplasms that proceed over a period of 4-5 years from low-grade tumors (diffuse or anaplastic astrocytoma's). Secondary gliomas are often identified in patients with a mean age of 39 years, have a slower growth rate, and have a better prognosis. De novo developing glioblastoma multiforme multiplies in 3 months. Although primary and secondary gliomas have different genetic origins and molecular growth routes, there are no physical variations between these two kinds (Urbanska *et al.*, 2014).

#### 2.2.1.2. Epidemiology

A critical public health issue, GBM is a rare tumor with a global incidence of less than 10 per 100,000 persons and a survival rate of 14–15 months after diagnosis. In all age categories, it accounts for 50% of all gliomas (Hanif *et al.*, 2017). GBM instances are 1-2 per 100,000 individuals in Europe and North America each year, with a 1.26:1 incidence rate in males. GBM instances affect children and newborns as well, with 1.1 to 3.6 cases per 100,000 newborns. The proliferative activity of glioma cells is related to differences. Caucasians are more likely to acquire

GBM, particularly in industrial locations, and there is a connection between genotype and tumor growth (Urbanska *et al.*, 2014).

The most frequent primary malignant brain tumor is glioblastoma (GBM). The current course of treatment is doing the maximum safe resection, then radiation with concurrent and adjuvant temozolomide. However, the overall survival rates at 2, 3, and 5 years are just 27%, 16%, and 9.8%, respectively. The inadequate local control following therapy is one of the key causes of this poor prognosis. Within 2 cm of the initial tumor, up to 77% of GBM recurrences occur, and 72% of cases occur in the radiation therapy zone (Yan *et al.*, 2019).

#### 2.2.1.3. Etiology

GBM's genesis is still not completely understood. Even though medical history mentions the emergence of glioma in related individuals, glioblastoma is believed to be a spontaneous tumor. In 1% of instances, the familial form of this tumor is documented. However, compared to glioblastomas that arise spontaneously, this type's genetic background is distinct (Nishihara *et al.*, 2015).

#### 2.2.1.4. Biological activity

The brain is where glioblastoma multiforme mostly develops. The brain stem and cerebellum, as well as the hemispheres, are subtly affected by this tumor. It is characterized by infiltrating growth, which makes it difficult to identify the tumor mass from normal tissue. A developing tumor increases intracranial pressure and can occasionally induce hydrocephaly (Manoranjan and Provias, 2011).

#### 2.2.1.5. Morphological features

GBMs contain very small cells that exhibit significant polymorphism, and anaplasia morphologically. Glioblastoma multiforme cells have ambiguous cellular borders, polygonal to spindle-shaped cells, and acidophilic cytoplasm. Their nuclei are oval or elongated, contain multiple discrete nucleoli that are centered or peri-centered, and have hyperchromatic chromatin that is coarsely clumped. In glioblastoma multiforme cells, there is nuclear pleomorphism and a greater ratio of the nucleus to the cytoplasm. Some cells include intranuclear inclusions. Binuclear and multinucleated cells, lymphocytes, neutrophils, macrophages, and necrotic cells may also be present (Zhen *et al.*, 2010).

Certain cells can imitate adipocytes and make up as much as 80% of some tumors, or between 5% and 10% of all tumor cells, due to the presence of enormous lipomatous vacuoles. This glioblastoma is referred to as a "fat-rich" glioma because although it has a distinct look, it has several molecular traits with a primary glioma (Urbanska *et al.*, 2014).

#### 2.2.1.6. Clinical symptoms

According to Baik et al., depending on the location and increasing intracranial pressure brought on by the disease's clinical stage, headaches, ataxia, dizziness, visual issues (blurred vision, diplopia), and recurrent syncope are the most common symptoms of GBM (Baik *et al.*, 2016).

Due to their ambiguous symptoms, gliomas are commonly misdiagnosed as infections, inflammatory diseases, and circulatory and immunological problems. A herniated lumbar disc may cause sciatica, back pain, and leg pain. Neuroimaging may also be required owing to a potential glioma if seizures begin in people who have not yet been diagnosed with epilepsy (Sanli *et al.*, 2010).

### 2.2.2. Current Methods of Diagnosing GBM Tumor

#### 2.2.2.1. Site

Nakada et al. showed cerebral hemispheres are the most common site for GBM; 95% of these tumors develop in the supratentorial area, while just a small percentage develop in the cerebellum, brainstem, and spinal cord (Hanif *et al.*, 2017).

The primary diagnostic technique for GBM is magnetic resonance imaging. The average tumor diameter at the time of diagnosis is around 4 cm, although data acquired by Simpson et al. (1993) showed that in 38% of 645 patients, the tumor diameter at the time of diagnosis was 5 cm, in 56% of cases it was within 5-10 cm, and in 6% of instances the tumor was > 10 cm. On MR imaging, the tumor (sometimes referred to as a "butterfly glioma") includes the corpus callosum and extends bilaterally into the occipital and temporal lobes (Opoku-Darko *et al.*, 2018).

The tumor or its components that were surgically removed are subjected to a histopathological evaluation utilizing conventional histological, cytologic, and histochemical techniques. A small needle aspiration biopsy is performed when it is not possible to remove a neurosurgical tumor (Zhen *et al*., 2010).

#### 2.2.2.2. Macroscopic and Histological Features of GBM

According to Ma et al. GBM exhibits regions of cystic and gelatinous tissue, necrosis, and multifocal bleeding on a macroscopic level (Ma *et al*., 2013). Hanif et al. show the variance in the tumor's gross appearance from one place to the next is a distinguishing trait of GBM. While certain tumor sites are solid and white and some sections have noticeable cystic degeneration and bleeding, some locations with tissue necrosis seem mushy and yellow in color. Typically, the tumor appears as a single, moderately big, irregularly shaped lesion that typically develops in the white matter (Hanif *et al.*, 2017).

GBM has many histological characteristics with anaplastic astrocytoma, including a pleomorphic cell population that varies in size from tiny, poorly differentiated tumor cells to giant, multinucleate cells with widespread necrosis, pseudo palisading nuclei, and abundant mitotic activity. Another important aspect is the proliferation of vascular endothelial cells, which typically have a glomeruloid shape (Ma *et al.*, 2013).

#### 2.2.2.3. Genetic and Molecular Pathogenesis

Based on standards established by the WHO, morphological diagnoses are made. The morphology, malignancy (grade I–IV), proliferative index, response to treatment, and survival time of central nervous system cancers are used to stage them. Non-malignant tumors are classified as grade I,

comparatively non-malignant tumors as grade II, low-grade malignant tumors as grade III, and most malignant tumors as grade IV, with a median survival of 6 to 12 months. The grade of glioblastoma multiforme is IV (Bhaskaran *et al*., 2020).

### 2.2.3. GBM Tumor and Other Tumors

Glioblastoma and brain metastases (BM) are the two most frequent malignant tumors of the adult central nervous system. A history of known primary neoplasms and the presence of many brain lesions are the two most important pieces of evidence utilized to make the diagnosis of metastasis. Although BM might be the first symptom of an unexplained extracerebral malignancy, roughly 40 to 50 percent of BM begin with a single lesion (Nayak *et al.*, 2012).

Glioblastoma (GBM) can also manifest in individuals with concurrent systemic cancer. On conventional magnetic resonance imaging (MRI), these two conditions often exhibit similarities, such as core necrosis, inhomogeneous ring enhancement, and surrounding edema. Consequently, while radiological differentiation is vital for informing patient management and prognosis, it can be a complex task due to the resemblance between these lesions (Hauser and Matthes, 2017).

A study by Romano et al. Although GBM and BM have comparable conventional magnetic resonance imaging, they differ greatly histopathologically. Both cells from the main location of systemic cancer and those from brain metastases are absent from the blood-brain barrier (BBB). Peripheral vasogenic edema is caused by a markedly enhanced capillary permeability because of this capillary ultrastructure, which also helps the metastases multiply quickly (Romano *et al.*, 2022).

However, GBM has a high rate of neo-angiogenesis, and its capillary ultrastructure resembles that of healthy brain tissue. Additionally, GBM histology analyses revealed that tumor cells had spread across the peritumoral region. As a result, infiltrative edema is a better way to define peritumoral edema in GBM (D'Alessio *et al.*, 2019).

To distinguish between GBM and BM, morphometric parameters and MR signal aspects of the tumoral mass and peritumoral area assessment were suggested. According to the authors, the existence of GBM may be established by the fact that the maximum diameter of the augmenting mass area is smaller than the largest diameter of the peritumoral region as measured on T2-weighted images (Romano *et al.*, 2022).

In adults, primary glioblastoma multiforme (GBM) and intracranial metastases are the most often diagnosed brain tumors. As their imaging properties and contrast-enhancement patterns are frequently identical, conventional magnetic resonance (MR) imaging of glioblastomas and isolated cerebral metastatic lesions may be unable to discriminate between these two entities.

To improve treatment planning, these lesions may be distinguished before surgery. (Tsougos *et al.*, 2012). Non-neoplastic lesions include demyelinating lesions that, based on conventional imaging, may seem to be brain tumors (such as tumefactive demyelination), infectious (including abscess), ischemia-related, or infectious lesions. It could be difficult to distinguish between malignant and non-cancerous tumors using a traditional MRI. Although MRI is a sensitive method of diagnosing brain lesions, its ability to differentiate between benign and malignant lesions is restricted. There may not be a mass effect in many non-neoplastic lesions, such as low-grade gliomas and early-stage or diffusely infiltrating lesions. Because they contain tiny T2 hyperintense

lesions, low-grade gliomas may be challenging to distinguish from isolated cortical dysplasia or other diseases (Donahoe, 2012).

Given that various non-neoplastic disorders are frequently linked to disturbance of the blood-brain barrier and not all tumors improve, the addition of a contrast agent may not boost diagnostic specificity (Gharzeddine *et al.*, 2019).

Conventional magnetic resonance (MR) imaging of glioblastomas and isolated cerebral metastatic lesions may be unable to differentiate between these two entities since their imaging characteristics and contrast-enhancement patterns are usually similar. In a traditional MRI, both of them show ring enhancement. These lesions may be identified before surgery to enhance treatment planning (Tsougos *et al.*, 2012).

### 2.2.4. Treatment of GBM Tumor

Despite several multinational initiatives, treating GBM continues to be the most difficult undertaking in clinical oncology. A variety of various therapies have been researched over the past ten years with very few results.

Hanif et al founded the location of the illness and its complicated and varied biology are the main obstacles to treating GBM. Although the survival and quality of life of GBM patients have gradually improved thanks to advancements in surgical techniques, radiation, and adjuvant chemotherapy, the prognosis is still dismal. To achieve favorable results, comparable to those in several other tumors that are already effectively treated, considerably more significant progress must be made (Hanif *et al.*, 2017).

#### 2.2.4.1. Surgery

The main element of routine treatment is surgery. Surgery can reduce tumor burden, regulate seizures, reverse neurological deficits, introduce local therapeutic agents, and enhance the quality of life, depending on the kind of tumor. The location and eloquence of the affected brain region determine the amount of surgical excision. Relapse happens in around 80% of cases, often within 2-3 cm of the margin of the initial lesion and is caused by the fact that GBM is a locally extremely invasive tumor that cannot be entirely cured by surgery. However, the degree of surgical resection maintains predictive value in cases of newly diagnosed individuals (Ohka *et al.*, 2012).

#### 2.2.4.2. Radiation Therapy

Radiotherapy can be used after surgery to eradicate any leftover tumor cells. Brachytherapy and stereotactic radiosurgery have been reported to be effective treatments against recurrent GBM, although they have hazy roles in treating freshly diagnosed GBM. This has been demonstrated to enhance the life expectancy of patients with high-grade gliomas. Following stereotactic radiotherapy, subgroups of patients who underwent a large complete resection could benefit in terms of survival. Hyperfractionated radiation, on the other hand, has demonstrated that survival results in GBM may be negative in some patient subgroups. Radiation therapy has several drawbacks and risks, including radio-resistance of certain tumors, radiation necrosis, radiation-induced persistent neural damage, and the invasive nature of GBM (Mukherjee *et al.*, 2014).

### 2.2.4.3. Chemotherapy

Several chemotherapeutic drugs have been evaluated for their efficacy in the treatment of GBM to increase patient survival. Out of them, alkylating drugs like temozolomide (TMZ), carmustine (BCNU), and lomustine (CCNU) have demonstrated some benefit and have been utilized therapeutically in the majority of GBM cases (Hanif *et al.*, 2017).

### 2.2.4.4. Current Treatment Options

The blood-brain barrier (BBB), a highly selective semipermeable barrier that separates blood from the brain, poses special difficulties for the treatment of brain tumors. The endothelial cells of capillaries, the astrocytes that surround the capillary, and the pericytes that are embedded in the capillary basal lamina make up the BBB. The capacity of a molecule to traverse the BBB is influenced by physiochemical characteristics such as molecular weight, lipophilicity, and charge.

The BBB blocks 98% of small-molecule medications and virtually all big molecules (>400 Da) from entering the central nervous system (CNS). If applicable and safe to do so, the current treatment protocol starts with surgically removing the tumor, then is followed by radiation and concurrent chemotherapy (Xu *et al.*, 2015).

Maximal resection during surgery is related to prolonged progression-free survival (PFS) and overall survival (OS), which is the first treatment option for GBM. Since resection is not a curative procedure, patients often also get chemotherapy and radiation. PFS and OS are both improved when radiotherapy, at a total dosage of 60 Gy, is used either as a main treatment or as a follow-up

after surgery. In patients with newly diagnosed GBM, concurrent treatment of temozolomide [150-200 mg/m2/day for 5 days each 28-day cycle], an oral alkylating drug, enhances OS from 12.1 months with radiation alone to 14.6 months with radiotherapy + temozolomide. Despite this improvement in survival with radiation plus temozolomide, tumor growth, and recurrence usually happen as a result of the emergence of temozolomide resistance. Patients' treatment choices are constrained after a GBM recurrence. Recently, the FDA-approved therapy for both recurring and newly diagnosed GBM has emerged: tumor treating fields (TTF), which administer electric fields to the tumor site to interrupt cancer cell proliferation. To enable the creation of innovative targeted medicines, it is necessary to identify new targets **(Taylor *et al.*, 2019).**

#### 2.2.4.5. Emerging Targeted Therapies

Given its invasive nature and characteristics of neo-angiogenesis and intratumor heterogeneity, GBM has a dismal prognosis. Several genetic and epigenetic changes in GBM affect the prognosis of the patient. Despite this heterogeneity, a comprehensive analysis of genetic aberrations in GBM found that three main signaling pathways are frequently dysregulated: activation of the receptor tyrosine kinase (RTK)/Ras/phosphoinositide 3- kinase (PI3K) pathway (88%), inhibition of p53 (87%), and retinoblastoma protein (Rb) signaling pathways (78%). Potential targeted therapeutics for GBM have been researched using medications that target many of these frequently found changes (Kim *et al.*, 2015).

### 2.2.5. MR Spectroscopy Technique

#### 2.2.5.1. Definition of MRS

For the non-invasive evaluation of brain metabolism, magnetic resonance spectroscopy (MRS) and the related method of magnetic resonance spectroscopic imaging (MRSI) are often employed in both clinical and preclinical research. Although their final clinical significance is still up for debate, they are also employed in medical practice. This chapter examines the standard MRS and MRSI methods as well as the overall informational nature of brain spectra.

Magnetic resonance spectroscopy (MRS) of the human brain has improved fast since its first discovery in the 1980s. The 31P nucleus was the focus of early studies in both humans and animals, allowing for the detection of phosphocreatine and adenosine triphosphate (ATP) as well as inorganic phosphate and phosphodiester, two energy-related metabolites (Duong, 2012).

Due to improved methods for spatial localization and water suppression, proton MRS became more and more popular in the 1990s due to its higher sensitivity and convenience (since, unlike MRS of other nuclei, it can be performed without hardware modification on most MRI machines). The proton is employed in the great majority of in vivo brain MRS research, even though nuclei like 31P, 23Na, and 13C continue to be significant, particularly at high magnetic field strengths (especially for isotopically tagged and/or hyperpolarized molecules). As a result, the next sections of this work focus on the 1H- MRS method (Green *et al.*, 2012).

#### 2.2.5.2. Brain proton MR spectrum information content

Due to their low sensitivity, in vivo, MR spectra frequently only reveal the presence of small, mobile molecules at millimolar concentrations. At long echo times (e.g., 140 or 280 ms) at commonly used field strengths of 1.5 or 3.0 T, only signals from choline (Cho), creatine (Cr), and N-acetyl aspartate (NAA) are visible in normal brain, whereas substances like lactate, alanine, or others may be detectable in pathological conditions which increase their concentration. Short echo durations (35 ms or fewer) allow the detection of several compounds, including lipids, macromolecular resonances, glutamate, glutamine, and myoinositol (Rahimian *et al.*, 2013).

## The major chemicals' biological importance

#### 2.2.5.2.1. N-Acetyl aspartate

The largest signal in the typical adult brain spectrum is NAA, which resonates at 2.01 part per million (ppm) as shown in figure 2.1. N-acetylaspartylglutamate (NAAG), which resonates at 2.04 ppm, contributes very little and is often unresolved. One of the amino acids that are most prevalent in the central nervous system is NAA. It has been hypothesized to be an osmolyte, a breakdown product of NAAG (which, unlike NAA, is a neurotransmitter), a source of acetyl groups for lipid synthesis, a regulator of protein synthesis, a storage form of acetyl-CoA or aspartate, or a storage form of acetyl-CoA or aspartate. In the mitochondria of neurons, aspartate and acetyl-CoA are converted into NAA (Rosso *et al.*, 2017).

As immunocytochemical investigations have indicated that NAA is mostly localized to neurons, axons, and dendrites within the central nervous system, NAA is frequently referred to as a "neuronal marker." However, according to other investigations, NAA may also be present in nonneuronal cells such as mast cells or isolated oligodendrocyte preparations. All things considered, NAA does appear to be a trustworthy surrogate marker of neuronal health, even though it occasionally varies regardless of the density or function of neuronal cells (like with other surrogate indications) (Moffett *et al.*, 2014).

#### 2.2.5.2.2. Choline

The "choline" signal ("Cho," 3.20 ppm) as shown in figure 2.1 is a composite peak made up of contributions from the glycerophosphocholine (GPC), phosphocholine (PC), and a little amount of free choline itself. These substances contribute to membrane production and breakdown, and they are frequently enhanced in diseases that entail higher membrane turnover rates (e.g., tumors). Cho levels in glial cells have also been shown to be elevated. Active demyelination, which may be caused by inflammation or by myelin phospholipids degrading predominantly to GPC, is another pathogenic mechanism that raises Cho. Decreased brain Cho levels have been seen in cases of hepatic encephalopathy, and some data points to the possibility that dietary choline consumption might alter cerebral Cho levels (Duong, 2012).

#### 2.2.5.2.3. Creatine

The "creatine" methyl resonance ("Cr," 3.03 ppm) as shown in figure 2.1 is a composite peak consisting of both the amino acids creatine and phosphocreatine, which are employed in the

creatine kinase reaction, which generates ATP, in the metabolism of energy. At 3.91 ppm, a resonance from creatine's CH2 may also be seen. In vitro, the concentration of creatine in glial cells is two to four times greater than that in neurons. Creatine also exhibits significant regional differences, with the cerebellum having far higher levels of Cr than supratentorial areas and white matter in the normal brain having lower amounts than gray matter (Bertholdo *et al.* 2013).

#### 2.2.5.2.4. Lactate

The lactate resonance, which is a doublet with a 7 Hz coupling constant centered at 1.31 ppm as shown in figure 2.1, is frequently undetected in a healthy brain. However, when lactate is present, MRS commonly detects pathogenic conditions such as acute hypoxia or ischemia damage, brain tumors, or mitochondrial diseases (Ru *et al.*, 2013).

#### 2.2.5.2.5. Myo-inositol

Myo-inositol (MI) is one of the largest signals in short echo time spectra, occurring around 3.5–3.6 ppm as shown in figure 2.1. The inositol triphosphate intracellular second messenger system includes the pentose sugar MI. It has been demonstrated that glial cells in vitro contain more MI than neurons. Alzheimer's dementia and demyelinating disorders have been linked to increased MI, whereas hepatic encephalopathy has been linked to decreased MI (Ciurleo *et al.*, 2014).

#### 2.2.5.2.6. Less Commonly Detected Compounds

Proton spectra of the human brain have identified about 25 new substances. Several of these substances are found in the typical human brain, but regular detection is challenging due to their tiny size and/or overlapping peaks. These include but are not limited to, NAAG, aspartate, taurine, Scylla-inositol, betaine, ethanolamine, purine nucleotides, histidine, glucose, and glycogen. Some compounds are much more difficult to discover, requiring the use of "spectral editing" techniques (Duong, 2012).

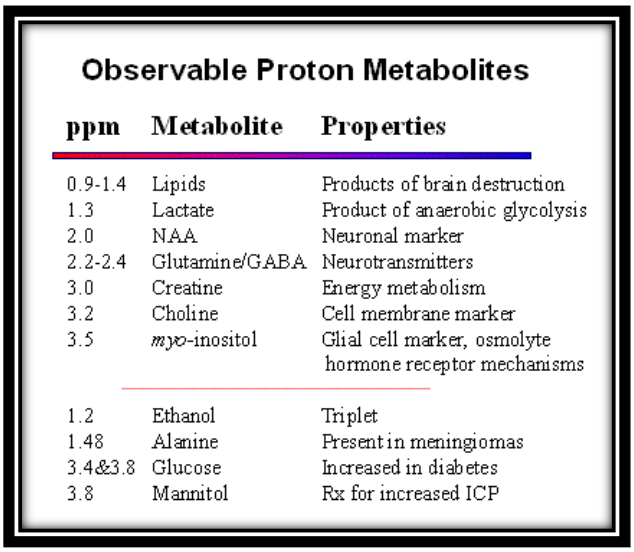


**Figure 2.1:** Observable Proton Metabolites (Network, 2014)

### 2.2.5.3. Spatial Localization Techniques

#### 2.2.5.3.1. Single-Voxel Techniques

Almost all single-voxel localization methods choose a signal from the area (“voxel") where they cross using three orthogonal slice-selective pulses as shown in figure 2.2. By using "crusher" field

gradient pulses, "phase-cycling," outer-volume suppression pulses, and alternating the phases of the slice-selective pulses and receiver, signals from outside the voxel are suppressed. For human brain spectroscopy, typical voxel sizes range from 4 to 8 $cm^3$ (Weinberg *et al.*, 2021).

A "stimulated echo" is produced by the "STEAM" sequence using three 90°pulses as shown in figure 2.2, whereas a "spin echo" is produced by the "PRESS" sequence using one 90°and two 180°refocusing pulses as shown in figure 2.3. The distinctions between STEAM and PRESS have been explored in great detail; perhaps the most important one is that the spin-echo-based PRESS sequence, which is commonly preferred, has twice the signal of STEAM. However, STEAM has the potential to provide shorter echo times, better slice profiles, and 90° pulses with a wider bandwidth. At high field strengths, STEAM may be especially beneficial for brain MRS in this way (e.g., above 3 T). While long TE PRESS (with its greater SNR) should often be employed for resonances with longer T2 , short TE STEAM may be preferred for studying resonances with shorter T2 (such as Cho, Cr, NAA, and lactate) (Ekici *et al.*, 2020).

There are major technological challenges associated with in vivo MRS with high field strengths (e.g., 3 T or more). It is difficult to produce uniform RF transmit (B1) fields, for example, due to wavelength effects in volume RF coils or the use of inhomogeneous surface coils for excitation. In any case, it may be difficult to get the correct flip angles in PRESS or STEAM, and the flip angles may change inside the voxel, resulting in signal loss (Weinberg *et al.*, 2021).

Since apparent metabolite T2 relaxation times are significantly shorter at extremely high fields for human MRS, such as 7 T, it is preferred to lower the TE of the localization sequence as much as is practical. A localization technique called "SPECIAL" (spin-echo full-intensity acquired

localized spectroscopy) combines beneficial traits like the entire signal intensity of PRESS with the shorter TE of STEAM (Weinberg *et al.*, 2021).

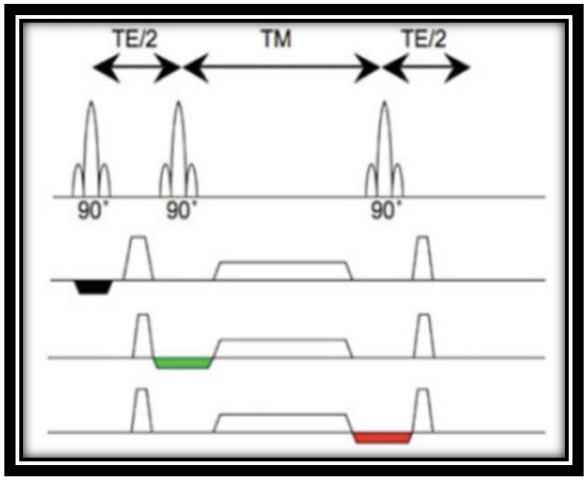


**Figure 2.2:** The STEAM sequence (three 90°) (Duong, 2012)

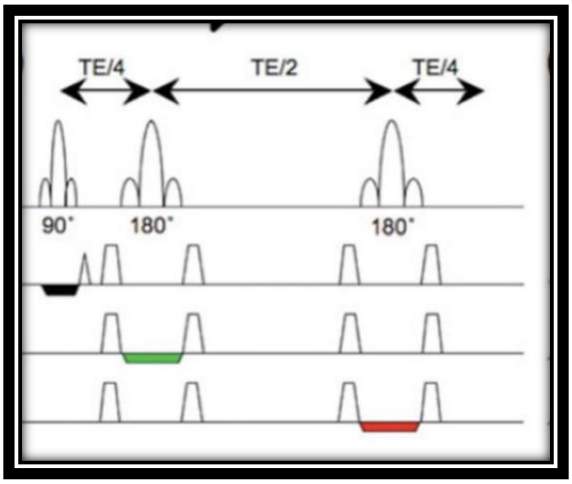


**Figure 2.3:** The PRESS sequence (90° and two 180°) (Duong, 2012)

### 2.2.5.3.2. Multiple-Voxel (MRSI) Techniques

While single-voxel MRS is rapid and simple to perform in most areas of the human brain, it is often only used in one or two brain regions in clinical research and offers no information on the

spatial changes of metabolites. MRSI, on the other hand, may be used to assess numerous voxel sites at once but is often more time-consuming.

Most frequently, MRSI is based on phase-encoding in two directions together with PRESS sequence-based signal excitation in a specific area as shown in figure 2.4. This allows B0 field homogeneity to be set on the specific region of interest, while also limiting the number of phase-encoding steps necessary for a given spatial resolution and preventing the stimulation of scalp lipid signals (Duong, 2012).

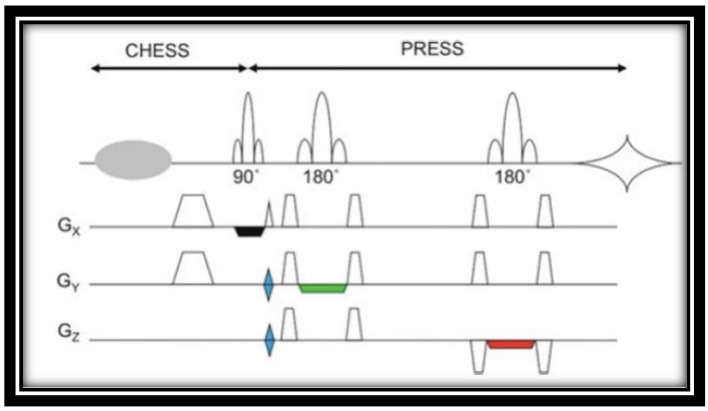


**Figure 2.4:**2D-PRESS-MRSI pulse sequence (Duong, 2012)

PRESS-MRSI does not provide multislice acquisitions, and the rectangular shape of the PRESS excitation makes it difficult to reach the boundaries of the brain. These drawbacks include inaccurate spectra at the PRESS box's edges caused by incorrect slice profiles of the 180° pulses. An alternative technique uses a slice-selective spin-echo sequence that may be used in multi-slice mode and excites the whole transverse slice as shown in figure 2.5. There are often many, precisely spaced outer volume suppression (OVS) pulses before the spin-echo sequence, in addition to the

regular water suppression pulses, to suppress the lipid signals from the scalp. MRSI with broad geographical coverage is often done at long echo times to reduce artifacts caused by residual water and lipid as well as field inhomogeneity (e.g., 140 or 280 ms) (Kalra, 2019).

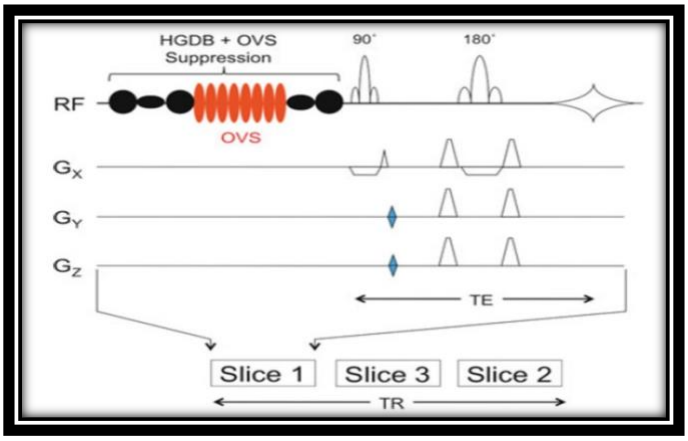


**Figure 2.5:** A multi-slice 2D-MRS pulse sequence (Duong, 2012)

The multi-slice strategy can cover the whole brain with a substantial number of slices, but the resulting scan time could be too long when utilizing conventional phase-encoding techniques. The pulse sequence for each slice must be as long as 0.5-1.0 s, covering all RF pulses and the data-collection window, to attain adequate spectral resolution. A TR that is too long and results in lengthy scan periods may be produced by interspersing four or five of these slices. On the other hand, if extensive brain coverage is needed, 3D-PRESS-MRSI can potentially result in very long scan periods. Field of view (FOV) divided by required spatial resolution equals the number of phase-encoding steps (N) (N = FOV/ spatial resolution). Consequently, it is crucial to specify a FOV as tiny as feasible bound only by the size of the object to be photographed to reduce the scan time (i.e., minimize N) while maintaining the appropriate spatial resolution. As the brain (which

is often oval in form) is smaller in this dimension, the left-right FOV should be less than the anterior-posterior FOV in the case of brain imaging. A reduced FOV in the left-right direction may often reduce scan time by an additional 25–30%. When wide FOVs and high resolutions in all three dimensions are required, fast MRSI techniques are typically utilized. Typically, if broad FOVs and high resolutions are required in all three dimensions, rapid MRSI methods are required to preserve clinically tolerable scan durations (Hangel *et al.*, 2022).

#### 2.2.5.4. Water and Lipid Suppression

The brain metabolites found by MRS are in the millimolar concentration range, whereas brain water is around 80 M. The tissue of the scalp is also shown to contain significant amounts of lipids. For the precise observation and measurement of brain metabolites, effective water suppression (and lipid suppression for MRSI) is required.

The most widely used method for water suppression employs frequency-selective saturation pulses called chemical shift suppression ("CHESS") to saturate the water signal before the localization process. Multiple CHESS pulses may be used for a variety of transmit B1 values and water T1 relaxation times to produce great suppression factors with ideal flip angles and delays (this is crucial for the suppression of both brain water and CSF) (Hassan *et al.*, 2019).

There are three common methods for lipid suppression. The use of spatial outer-volume suppression (OVS) pulses is one way to reduce lipid signals in the scalp as shown in figure 2.5. Alternately, an inversion recovery strategy may be applied, which benefits from the difference in T1 values between metabolites (usually 1,000–2,000 ms at 1.5 T) and lipids (about 300 ms at 1.5 T). At 1.5 T, an inversion duration of 200 ms (= T1 * ln) will mostly keep the magnetization of the metabolite inverted while preferentially nullifying the lipid signal. Because no assumptions are

made regarding the spatial distribution of the lipid, this technique can suppress lipid signals everywhere in the brain, although it may slightly lower metabolite SNR (Hassan *et al.*, 2019).

#### 2.2.5.5. MR Spectroscopy Mechanism

It was found early on in the development of human brain proton MRS that the spectra of healthy brain tissue and brain malignancies were notably different. Most brain cancers had decreased N-acetyl aspartate (NAA) signals, and many also had increased choline (Cho), which resulted in increased Cho/NAA ratios as shown in figure 2.6. Because that NAA is thought to be predominantly of neuronal and axonal origin, the reduction in NAA is frequently interpreted as the loss, malfunction, or displacement of normal neural tissue. The choline-containing chemicals that are involved in membrane production and degradation contribute to the 'Cho' signal, which is made up of a variety of them. It has been hypothesized that the enhanced choline signal in brain tumors results from higher membrane turnover. According to in vitro research, brain tumors' higher Cho signal is caused by an increase in phosphocholine levels (Pcho). Cho has also been discovered to have a strong correlation with the tumor's cellular density and the depth of the tumor's invasion into the brain. Hence, it has been suggested that one technique for establishing tumor borders in treatment planning is to employ MRSI to map Cho levels (Donahoe, 2012).

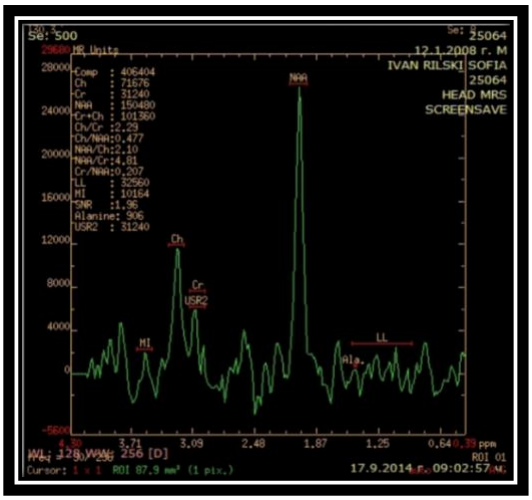


Metabolite Ratios

| | Normal | Abnormal |
|---|---|---|
| NAA/Cr | 2.0 | < 1.6 |
| NAA/Cho | 1.6 | < 1.2 |
| Cho/Cr | 1.2 | > 1.5 |

**Figure 2.6:** MR spectrum (Pacheva *et al.*, 2016) & metabolite ratios (Haider *et al.*, 2012)

Increased signals in the lactate and lipid portion of the spectrum, as well as occasionally higher levels of myoinositol (MI) in short echo time (TE) spectra, are other somewhat typical metabolic alterations in human brain tumors. The rise in lactate is most likely the consequence of anaerobic glycolysis, although it may also be caused by ischemia from inadequate blood supply or necrosis. It is thought that the presence of increased lipid levels is related to membrane breakdown and necrosis. High levels of MI are thought to be a reflection of more glial cells, which have been found to contain high quantities of MI and are more prevalent in grade II gliomas than other gliomas. Moreover, even in the absence of high Cho, individuals with gliomatosis cerebri have been observed to have elevated inositol levels (Donahoe, 2012).

## 2.3. Literature Review

### 2.3.1. The Effectiveness of The MRS Technique in Diagnosing GBM Tumor.

MRI, a reliable method for identifying GBM tumors, allows for anatomical imaging of the brain tumor. In MRI imaging, GBMs are shown as ring-enhancing lesions. However, this pattern can

also be seen in abscess, metastasis, and tumefactive multiple sclerosis and is not limited to GBM. The spatial spread of cancerous cells in the brain cannot be detected by MR methods, despite the great contrast of soft tissue in MRI images for the site of the GBM tumor. Any sort of treatment, including surgery, chemotherapy, or radiation, requires the capacity to discern between tumor-free and healthy areas (Diego *et al.*, 2015).

It is necessary to pinpoint the tumor's exact position, which necessitates a thorough knowledge of brain tissue. Brain tissue metabolite concentrations such phosphocholine (Pcho), creatine (Cr), and N-acetyl aspartate (NAA), as well as concentration ratios like NAA/Cr and Pcho/Cr, are affected by neurological diseases. Non-invasive proton magnetic resonance spectroscopy (1HMRS) may be used to determine the metabolic profile of brain tissue, including the concentration and distribution of metabolites (Crain *et al.*, 2017). MRS is a clinical tumor assessment tool that has been used to assess a variety of brain tumor forms. According to research by Einstein et al. for patients with (Pcho/NAA) > 1.1, stereotactic radiosurgery outlives conventional therapy (Einstein *et al.*, 2012).

Haaga et al. showed (Gln) first described glutamine, NAA, Pcho, glutamic acid (Glu), and other important brain metabolites. Particularly significant for neurological diseases, notably brain tumors, is the NAA metabolite. Furthermore, they discovered that the NAA/Cr and Pcho/Cr ratios altered in GBM tumors in a way that contrasted with healthy brain tissue (Mansoory *et al.*, 2020). According to Parra et al., the distribution of metabolites like NAA and Pcho in healthy and tumoral voxels varied significantly. Tumoral voxels displayed greater levels of Pcho and lower levels of NAA compared to healthy voxels (Parra *et al.*, 2014). By analyzing MRS data, Crain et al. found

that five ratios—Pcho/Cr, Cr/Pcho, NAA/Pcho, Lac/Lip, and Pcho/NAA—help to discriminate between healthy and tumoral voxels in GBM (Crain *et al.*, 2017).

Although its precise role is unknown, NAA is widely accepted as a marker of functioning neurons and their appendages. Any damaging, degenerative, or infiltrative process that damages or destroys normal brain tissue results in a noticeable drop in NAA. NAA is significantly decreased due to the typical brain damage caused by GBM lesions (Tsougos *et al.*, 2012) .

The concentration of metabolites in MRS signals has been quantified using a variety of approaches, however, the quantifications are still subject to large fluctuations and inaccuracies (Dezfouli *et al.*, 2017). Recent research has demonstrated that by utilizing MRS multivoxel data, unknown metabolites or ratios may need to be assessed for GBM tumors. These ratios and their metabolites were studied (Mansoory *et al.*, 2020).

Conventional MRI is unable to differentiate between these two forms of intracerebral lesions because their neuroimaging appearance is typically comparable, unclear, or identical. Magnetic resonance spectroscopy (MRS), one of the MR methods, is starting to become important in classifying the majority of types and grades of brain tumors. Quantifying indicators of tumor metabolism, such as glucose, membrane turnover, and proliferation, such as choline (Cho), energy homeostasis, such as N-acetyl- aspartate (NAA), and necrosis, such as lactate (Lac) or lipids, has been done using advanced spectroscopic methods. MRS offers details on the make-up of metabolic tissue (Wang *et al.*, 2017).

Using multivoxel proton MR spectroscopy (1H-MRS), a choline (Cho)/N-acetyl aspartate (NAA) index was developed to gauge the survival of typical neurons and the rate at which cells are turned

over. GBM possesses atypical H-MRS characteristics that can be used to further isolate it from other peritumoral malignancies (Yan *et al.*, 2019) .

According to certain research, grade II or grade III astrocytoma had lower amounts of Cho than high-grade tumors, such as grade IV glioblastoma multiforme (GBM). This might be as a result of necrosis, which is linked to low levels of all metabolites and is present in high-grade tumors, especially those with necrotic cores. The spectra may differ significantly depending on the area that is sampled by MRS since tumors are frequently heterogenous, with necrotic cores, proliferative rims, and invasion of neighboring brain tissue. As a result, the region-of-interest selected for investigation will have a significant impact on the outcomes. As mentioned above, MRSI is often regarded as superior since it enables the evaluation of metabolic heterogeneity and the selection of the voxel with the highest Cho signal for study (Donahoe, 2012) .

# CHAPTER THREE

# METHODOLOGY

## 3.1 Introduction

In this chapter, the researcher presents subsequent sections, study design, study settings, study population, sample size, study instrument, data analysis method, scale correction, and ethical considerations.

## 3.2 Study design

The study was a quantitative descriptive cross-sectional interventional study to evaluate the glioblastoma multiform using MR Spectroscopy and the effectiveness of the MRS to dispense with a biopsy in the MRI department work practice of Palestinian governmental hospitals, especially in the Palestine Medical Complex (PMC) MRI department.

The study is an additional examination of the magnetic resonance image to reach a diagnosis of GBM disease to dispense with the surgical procedure to obtain a biopsy. Information was collected in the period between the October 2022 to June 2023.

## 3.3 Study Setting

The study setting was at the MRI department at the Palestine Medical Complex in Ramallah Palestine, and all patients diagnosed with GBM, and patients suspected of having the GBM were included.

## 3.4 Study Population and sample size

The study population was all patients diagnosed with GBM tumors in the West Bank. The sample consisted of 7 patients with GBM (high-grade and low-grade tumors, neoplastic and non-neoplastic GBM tumors) (2 patients new and 5 patients with tumor resection). It was be analyzed and studied in this research and applied to patients presented to the MRI department at the Palestine Medical Complex in Ramallah and 3 patients with another brain lesion (1 metastasis, 1 meningioma, 1 Oligodendroglioma) for comparison.

## 3.5 Study Instrument

In this study, the researcher used an intervention case study, it consisted of four parts:

Part one included Information about the patients studied and the number of normal and tumoral voxels for each patient about the demographic characteristics of the participants including case number, sex, age, normal voxel, and tumoral voxel.

The second part included the metabolism of brain tissue in the tumoral voxel and normal voxels The main MRS analyzed parameters of tumor and normal voxels including phosphocholine (Pcho), creatine (Cr), and N-acetyl aspartate (NAA), as well as concentration ratios like NAA/Cr and Pcho/Cr.

The third part included Significant correlations between different parameters of Tumor voxels.

The four parts included Diagnostic value analysis for significantly different data between tumor and normal voxel.

## 3.6 Ethical Considerations

The researcher obtained permission to conduct the necessary examination for the participating patients from the Palestinian Ministry of Health (Appendix A). The researcher also included an information sheet that defines the objectives of this study and confirms that participation is optional and that the participant's information will be kept confidential and used for scientific research purposes only (Appendix B). Patient privacy and confidentiality were protected, and participants were assured that they did not need to give out data such as name, address, or any other information that could be used to identify them.

After that, the consent of all patients was finalized, and their signatures were taken. The approval of the Scientific Research Ethics Committee at the Arab American University (IRB) was obtained (Appendix C). The approval of the facility for graduate studies of AAUP was obtained (Appendix D).

## 3.7 Data collection

A part of the study procedure was illustrated in figure 3.1.

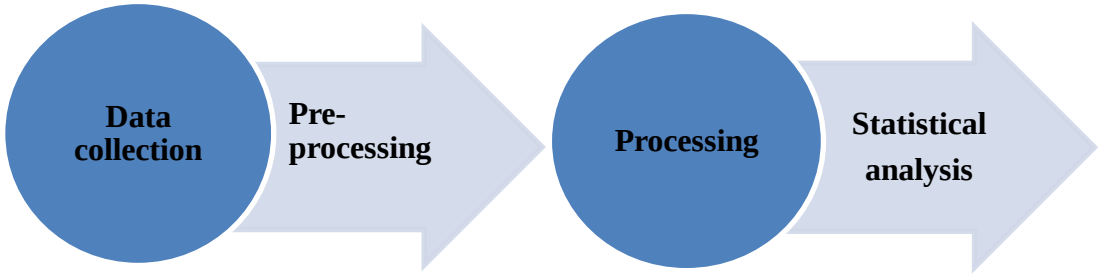


**Figure 3.1:** The study algorithm

### 3.7.1 Data collection

The MRI department of the Palestine Medical Complex in Ramallah, Palestine, collected data about 7 patients with GBM (2 patients new and 5 patients with tumor resection) (high-grade and low-grade tumors, neoplastic and non-neoplastic GBM tumors), 1 patient with Metastases 1 patient with Meningioma, and 1 patient with Oligodendroglioma from October 2022 to June 2023. Before scanning, each participant received a thorough explanation and signed ethical consent forms.

Also, the information was gathered by the Arab American University-Palestine, Dealership of Scientific Research, IRB committee's Medical Ethics Code (Code of Ethics: N/29/A/2023). Table 3.1 below contains demographic data about the patients who were the subject of the study. Figure 3.2 below has shown how differentiation between normal voxels and tumoral voxels.

This study employed multivoxel spectroscopic imaging with a 1.5-Tesla MRI scanner from the General Electric Corporation. Multivoxel spectroscopy was used to get an excellent spectrum from a big area. We used the Point-Resolved Spectroscopy [PRESS] imaging technique with

TE=144 ms, TR=1570 ms, and 1024 data points.

Before collecting data, a magnetic field shift was automatically carried out. When compared to short TE, the long TE utilized in this work has various advantages over short TE, including the ability to identify the NAA peak and Cr peak, and the Pcho peak and its ratio. Radiologist with a high level of experience in the analysis of MRS examinations used the individuals' MRS data to tag and regionalize tumoral and non-tumorous areas and compare GBM and other tumors.

**Table 3.1**. Details on the study subjects, including the number of normal and tumoral voxels for each subject.

| Case number | Sex | Age | Type of tumor | Normal voxel | Tumoral voxel | Total voxel |
|---|---|---|---|---|---|---|
| **1** | M | 57 | GBM | 3 | 12 | 15 |
| **2** | M | 58 | GBM | 18 | 17 | 35 |
| **3** | F | 59 | GBM | 13 | 8 | 21 |
| **4** | F | 45 | GBM | 3 | 12 | 15 |
| **5** | M | 71 | GBM | 7 | 8 | 15 |
| **6** | F | 55 | GBM | 3 | 12 | 15 |
| **7** | F | 60 | GBM | 12 | 9 | 21 |
| **8** | F | 57 | MANANGIOMA | 15 | 10 | 25 |
| **9** | M | 54 | METS | 8 | 7 | 15 |
| **10** | M | 36 | OLIGODENDROGLIOMA | 9 | 6 | 15 |

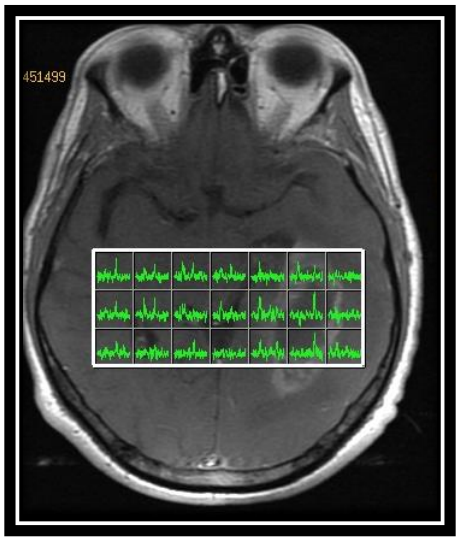


**Figure 3.2:** Illustrates the normal and tumoral voxels

### 3.6.2 Pre-processing

The data was pre-processed and the MRS range of imaging was identified using spectroscopy imaging visualization and computing (SIVIC), an open-source, standards-based software framework and application suite for processing and visualizing Digital Imaging and Communications in Medicine (DICOM), MR Spectroscopy data processing, and visualization. Then, the MR image was overlaid with the MRS image. Figure 3.3 reveals the target region at the end. The device's MRS signal is a transient sinusoidal signal that also contains the water signal, baseline signal, and residual signal (noise), among other undesirable components.

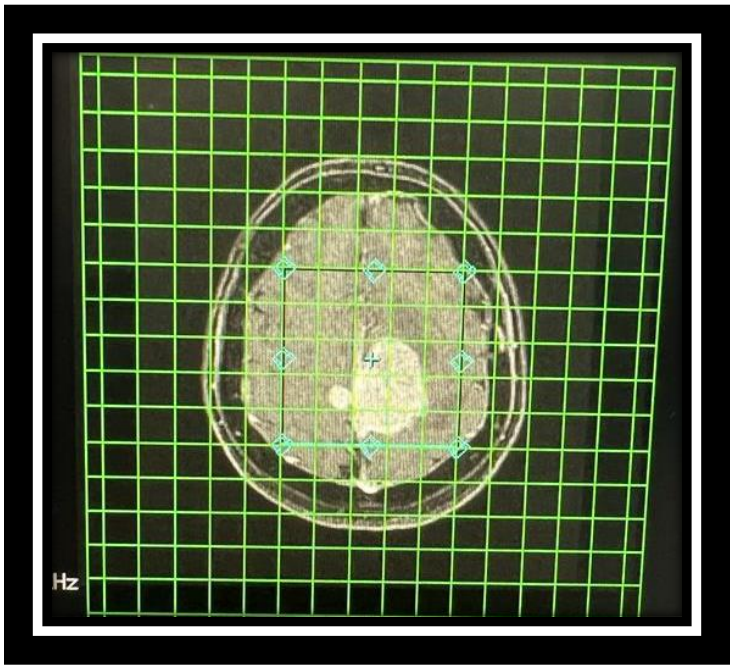


**Figure 3.3:** The image depicts a SIVIC-created MRI image, with a light green box representing the tumor area's perimeter and a square with a green tag representing each voxel.

S [t]=Met[t]+w[t]+Res[t] was used to define the primary signal received. S stands for the received signal, Met for the signal of metabolites, w for the signal of water, and Res for residual signals, which include noise and other things (Mansoory *et al.*, 2020).

Macromolecules are the source of the baseline signal, which first shows in the early phases of signal samples before quickly disappearing. The ambient signal is mellow. Similar to other MR imaging methods, the quality of the Res signal is impacted by several aberrations, including poor shimming, phasing errors, and chemical shift displacement. The major goals of the pre-processing stage are to identify metabolite signals among the main signal and precisely quantify those signals. The need to suppress the 10,000 times larger water signal is because the quantities of metabolites in brain tissue are substantially lower than those in water. In the current study, water suppression was done at a 45 Hz frequency.

Since the baseline signal hurts the number of other metabolites, it should be removed from the signal after water suppression to compute these values accurately, the water suppression was done with automated water suppression (AWS) by using Spectroscopic prep-scan.

### 3.6.3 Processing

Due to their capacity to be detected at an echo time (TE) of 144 milliseconds, the Pcho, NAA, Cr, Pcho/Cr ratio, Pcho/NAA ratio, NAA/ Pcho, and NAA/Cr ratio, as well as the Cr/NAA signals, have been chosen as the reference signals. This decision was made because it is possible to accurately detect and quantify these particular metabolites at this TE, assuring their usefulness as reference signals in the spectroscopic investigation.

### 3.6.4 Statistical analysis

By used the Kolmogorov-Smirnov test, the normal distribution of quantitative data was assessed for two different voxel types. The Independent Samples T-test was used to investigate the normal distribution of the data, and the Mann-Whitney U test was used to analyze the non-normal distribution. The probability of a correlation between the data in the patients' voxels was assessed using the Pearson test. Finally, by creating a ROC curve, the sensitivity and specificity of important analytes were calculated. The level of significance for each computation was set at p value 0.5. SPSS software version 16 was utilized to conduct statistical analysis for computed values from the previous step.

# CHAPTER FOUR

# RESULTS

## 4.1 Response Rate

In our study, 7 patients with glioblastoma multiform (GBM), 3 male and 4 female (2 patients new and 5 patients with tumor resection), 1 patient with metastases, 1 patient with meningioma, and 1 patient with Oligodendroglioma Table 3.1, were studied by MRS test, and tumoral voxels and normal voxels for GBM were analyzed, several normal voxels 59 and number of tumoral voxels 78 for GBM tumor, with response rate 87.5%. The results will thus apply to the study population because the response rate in this study was relatively high.

## 4.3 Data Analysis

For the total number of voxels of GBM, whether normal or tumoral, the level of metabolic ratio values of NAA/Cr, NAA/Pcho, Pcho /Cr, Pcho /NAA, and Pcho concentration, were (1.24 $\pm$ 0.68, 0.90 $\pm$ 0.54, 1.81 $\pm$ 1.11, 1.91 $\pm$ 2.08, 66999.17 $\pm$ 51226.74) respectively for the tumoral voxel and (2.34 $\pm$ 1.39, 1.67 $\pm$ 0.56, 1.49 $\pm$ 0.95, 0. 69 $\pm$ 0.34, 62585.15 $\pm$ 37676.36) respectively for normal voxel, the ratio of the tumoral voxel were significantly higher than the normal ratio, and the concentration of Pcho higher than the normal voxel as shown in table 4.1.

For the tumoral voxels of metastases, the metabolic ratio values of NAA/Cr, NAA/ Pcho, Pcho /Cr, Pcho /NAA, and Pcho concentration were (1.27 ± 0.50, 1.37 ± 0.86, 1.08 ± 0.35, 1.20 ± 1.17, 69322 ± 37608.88) respectively; for meningioma, the values were (1.92 ± 0.71,1.13 ± 0.67, 2.1 ± 1.25, 0.906 ± 0.80,33880 ± 31759.94) respectively, for Oligodendroglioma, the values were (1.169 ± 0.471, 1.07 ± 0.612, 1.313 ± 0.613, 1.33 ± 0.918, 57889 ± 33611.67) respectively as shown in

table 4.2.

**Table 4.1. The main MRS analyzed parameters of the tumor and normal voxels of GBM.**

| | Normal voxel | | | Tumoral voxel | | | Total | | |
|---|---|---|---|---|---|---|---|---|---|
| parameters | Mean | Median | Standard Deviation | Mean | Median | Standard Deviation | Mean | Median | Standard Deviation |
| Pcho | 62585.15 | 59664.00 | 37676.36 | 66999.17 | 50897.00 | 51226.74 | 65098.24 | 57772.00 | 45781.42 |
| Cr | 48286.66 | 45936.00 | 29309.51 | 49148.88 | 35640.00 | 49824.00 | 48777.56 | 40106.00 | 42095.56 |
| NAA | 97112.95 | 91176.00 | 57470.90 | 50382.85 | 38148.00 | 42832.33 | 70507.49 | 51480.00 | 54650.40 |
| Cr+Pcho | 104715.59 | 97800.00 | 61085.90 | 107494.74 | 83560.00 | 80426.56 | 106297.88 | 88720.00 | 72495.18 |
| Pcho/Crea | 1.49 | 1.19 | 0.95 | 1.81 | 1.48 | 1.11 | 1.67 | 1.37 | 1.05 |
| Pcho/NAA | 0.69 | 0.61 | 0.34 | 1.91 | 1.25 | 2.08 | 1.39 | 0.84 | 1.69 |
| NAA/Pcho | 1.67 | 1.63 | 0.56 | 0.90 | 0.82 | 0.54 | 1.23 | 1.20 | 0.67 |
| NAA/Cr | 2.34 | 1.97 | 1.39 | 1.24 | 1.21 | 0.68 | 1.71 | 1.56 | 1.18 |

**Table 4.2.** The main MRS analyzed the parameters of the tumor and normal voxels of another lesion.

| Parameter | Mets | | Meningioma | | Oligodendroglioma | |
|---|---|---|---|---|---|---|
| | Mean | Sd. | Mean | Sd. | Mean | Sd. |
| Pcho | 69322.00 | 37608.88 | 33880 | 31759.94 | 57889 | 33611.67 |
| Cr | 65013.14 | 27959.19 | 62550 | 28924.83 | 63400 | 39311.20 |
| NAA | 78829.71 | 39427.81 | 58096 | 39820.77 | 71136 | 62351.19 |
| Cr+Cho | 129291.43 | 69465.63 | 95360 | 56262.75 | 116053 | 65142.68 |
| Pcho/Crea | 1.08 | 0.35 | 2.1 | 1.25 | 1.313 | 0.613 |
| Pcho/NAA | 1.20 | 1.17 | 0.906 | 0.80 | 1.33 | 0.918 |
| NAA/Pcho | 1.37 | 0.86 | 1.13 | 0.67 | 1.07 | 0.612 |
| NAA/Cr | 1.27 | 0.50 | 1.92 | 0.71 | 1.169 | 0.471 |
| Cr/NAA | 1.04 | 0.84 | 0.66 | 0.59 | 0.998 | 0.438 |

The mean and standard deviation of the metabolic ratio within a normal and tumoral voxel of glioblastoma are summarized in Table 4.1. However, the level of Cr has no significant difference in the normal and tumoral voxels 48286.66 ± 45936.00, 49148.88 ± 49824.00 respectively. The results of the correlation analysis between different biochemical parameters in tumoral voxels are Creatine (Cr) and Pcho have a significant positive correlation of 0.479(P=0.00). Highly Significant Positive Correlation between Pcho and NAA 0.586(p=0.00). Pcho and Cr+ Pcho correlate 0.900 (very strong positive) (p=0.00). Pcho/NAA and NAA have a correlation coefficient of 0.696 (p=0.00), indicating a very significant positive association between the two variables. The positive result implies that a rise in one variable's (Pcho/NAA) value is substantially correlated with an increase in the other variable's (NAA) value. A significant positive correlation exists between the Pcho and Pcho/Crea Ratio of 0.395(p=0.00). The correlation between Pcho and Pcho/NAA Ratio is 0.272(p=0.001), which is significant. NAA/Pcho and Pcho have a significant negative correlation of -0.328(P=0.00). NAA/Cr: No Significant Correlation and Pcho(p=0.960). No

significant correlation between Pcho and Cr/NAA. NAA and creatine (Cr) have a significant positive correlation of 0.456(p=0.00). Cr+Cho and creatine (Cr) have a highly significant positive correlation of 0.625(p=0.00). Pcho/Crea Ratio and Creatine (Cr) have a significant negative correlation of -0.172(p=0.045). No significant correlation was found between creatine (Cr) and Pcho/NAA ratio (p=0.803) as shown in figure 4.1.

**Correlations**

| | | (Pcho) | Creatine (Cr) | (NAA) | Cr+Cho | Pcho/Crea Ratio | Pcho/NAA Ratio | NAA/cho | NAA/Cr | Cr/NAA |
|---|---|---|---|---|---|---|---|---|---|---|
| (Pcho) | Pearson Correlation | 1 | .479** | .586** | .900** | .395** | .272** | -.328** | 0.004 | -0.004 |
| | Sig. (2-tailed) | | 0.000 | 0.000 | 0.000 | 0.000 | 0.001 | 0.000 | 0.960 | 0.960 |
| | N | 137 | 137 | 137 | 137 | 137 | 137 | 137 | 137 | 137 |
| Creatine (Cr) | Pearson Correlation | .479** | 1 | .456** | .625** | -.172* | -0.022 | -0.055 | -0.144 | .185* |
| | Sig. (2-tailed) | 0.000 | | 0.000 | 0.000 | 0.045 | 0.803 | 0.524 | 0.093 | 0.030 |
| | N | 137 | 137 | 137 | 137 | 137 | 137 | 137 | 137 | 137 |
| (NAA) | Pearson Correlation | .586** | .456** | 1 | .614** | -0.039 | -.349** | .403** | .378** | -.399** |
| | Sig. (2-tailed) | 0.000 | 0.000 | | 0.000 | 0.654 | 0.000 | 0.000 | 0.000 | 0.000 |
| | N | 137 | 137 | 137 | 137 | 137 | 137 | 137 | 137 | 137 |
| Cr+Cho | Pearson Correlation | .900** | .625** | .614** | 1 | 0.125 | 0.142 | -.220** | -0.089 | 0.119 |
| | Sig. (2-tailed) | 0.000 | 0.000 | 0.000 | | 0.145 | 0.097 | 0.010 | 0.301 | 0.168 |
| | N | 137 | 137 | 137 | 137 | 137 | 137 | 137 | 137 | 137 |
| Pcho/Crea Ratio | Pearson Correlation | .395** | -.172* | -0.039 | 0.125 | 1 | .412** | -.413** | .377** | -.170* |
| | Sig. (2-tailed) | 0.000 | 0.045 | 0.654 | 0.145 | | 0.000 | 0.000 | 0.000 | 0.048 |
| | N | 137 | 137 | 137 | 137 | 137 | 137 | 137 | 137 | 137 |
| Pcho/NAA Ratio | Pearson Correlation | .272** | -0.022 | -.349** | 0.142 | .412** | 1 | -.632** | -.382** | .679** |
| | Sig. (2-tailed) | 0.001 | 0.803 | 0.000 | 0.097 | 0.000 | | 0.000 | 0.000 | 0.000 |
| | N | 137 | 137 | 137 | 137 | 137 | 137 | 137 | 137 | 137 |
| NAA/cho | Pearson Correlation | -.328** | -0.055 | .403** | -.220** | -.413** | -.632** | 1 | .510** | -.494** |
| | Sig. (2-tailed) | 0.000 | 0.524 | 0.000 | 0.010 | 0.000 | 0.000 | | 0.000 | 0.000 |
| | N | 137 | 137 | 137 | 137 | 137 | 137 | 137 | 137 | 137 |
| NAA/Cr | Pearson Correlation | 0.004 | -0.144 | .378** | -0.089 | .377** | -.382** | .510** | 1 | -.556** |
| | Sig. (2-tailed) | 0.960 | 0.093 | 0.000 | 0.301 | 0.000 | 0.000 | 0.000 | | 0.000 |
| | N | 137 | 137 | 137 | 137 | 137 | 137 | 137 | 137 | 137 |
| Cr/NAA | Pearson Correlation | -0.004 | .185* | -.399** | 0.119 | -.170* | .679** | -.494** | -.556** | 1 |
| | Sig. (2-tailed) | 0.960 | 0.030 | 0.000 | 0.168 | 0.048 | 0.000 | 0.000 | 0.000 | |
| | N | 137 | 137 | 137 | 137 | 137 | 137 | 137 | 137 | 137 |

**Figure 4.1**: Significant relationships between the various tumor voxel characteristics.

According to numerical values of the sensitivity and specificity of numerous tests in differentiating between tumoral and normal voxels, Pcho/NAA had the best diagnostic value with an Area Under Curve (AUC) of 0.836 (sensitivity 83.3% and 28.8%% specificity). The second effective test was Cr/NAA, which had an AUC of 0.787 (sensitivity: 78.2%, specificity: 35.6%). The third useful test was the Pcho/Crea Ratio, which had an AUC of 0.611 (sensitivity: 61.5%; specificity: 40.7%) as shown in figure 4.2 and table 4.3.

**Table 4.3**: Diagnostic value analysis for significantly different data of tumoral voxel

| Parameter | AUC | Cut-off | Sensitivity (%) | Specificity (%) |
|---|---|---|---|---|
| (Pcho) | 0.490 | 51095.0 | 48.7% | 59.3% |
| Creatine (Cr) | 0.452 | 41008.0 | 44.9% | 54.2% |
| (NAA) | 0.244 | 60324.0 | 24.4% | 69.5% |
| Cr+Cho | 0.479 | 90340.0 | 47.4% | 52.5% |
| Pcho/Crea | 0.611 | 1.3400 | 61.5% | 40.7% |
| Pcho/NAA | 0.836 | 0.7170 | 83.3% | 28.8% |
| NAA/Pcho | 0.152 | 1.4300 | 15.4% | 67.8% |
| NAA/Cr | 0.207 | 1.7450 | 20.5% | 64.4% |
| Cr/NAA | 0.787 | 0.5740 | 78.2% | 35.6% |

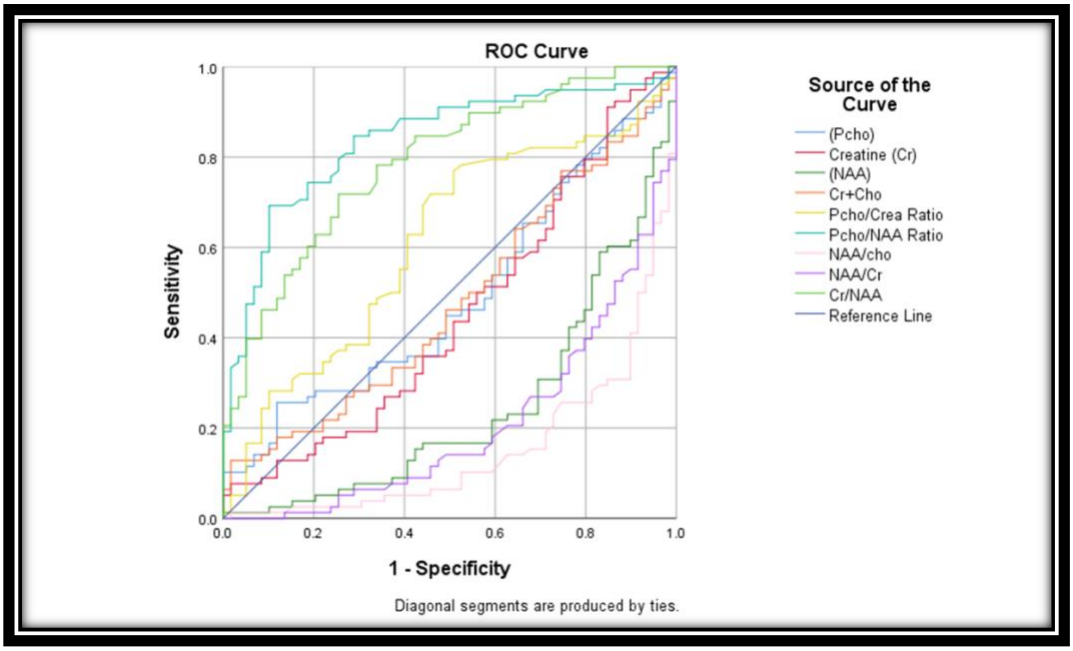


**Figure 4.2**: ROC curve for brain metabolites for different parameters of tumor voxels

## 4.4 Summary

This chapter included a description of the research results, including the characteristics of the tumoral voxel and the normal voxel of GBM tumor, as well as a description of the results of the tumoral voxel and the normal voxel of other tumors, as well as the results of the diagnostic values and showing the effectiveness of the examination.

# CHAPTER FIVE

# DISCUSSION & CONCLUSION

## 5.1 Introduction

This section covers the study's discussion about the causes and how they differ from earlier local and international studies. This chapter also includes the study's conclusion, suggestions, strengths, weaknesses, and areas for further research.

## 5.2 Discussion

Through the simultaneous analysis of multiple studies in a mix of healthy and tumoral voxels, the diagnostic value of detectable metabolites in long TE was evaluated in this study for the first time in Palestine. According to our findings, healthy voxels had considerably greater levels of Cr, NAA, and NAA/Cr than tumoral voxels. In contrast, tumoral voxels had considerably greater Pcho/Cr, Pcho/NAA ratios, and Pcho concentrations than healthy voxels.

Various diseases can be diagnosed using various biochemical analyses. A biomarker is a biological molecule that may be evaluated using a specific methodology to identify a pathologic process or a patient's reactions to a treatment substance (Kohler *et al.*, 2017).

According to the findings of Verma et al., the Pcho/NAA ratio increased in glioblastoma about the degree of malignancy (Verma *et al.*, 2016). They were able to find nonetheless, that non-neuroectodermal malignancies had lower total Cr concentrations. In contrast to normal voxels, we found higher concentrations of Pcho and lower levels of Cr in tumor voxels.

However, in glial tumors or meningotheliomatous meningiomas, Cr levels drop by 15–40%. Additionally, total Cr content in brain metastases is substantially lower than in neuroectodermal malignancies. Cr is a crucial metabolite of cellular energy metabolism. Despite some pathological reactions affecting the central nervous system being stable, glioblastoma and astrocytoma's usually cause them to decline. Increased metabolism in tumor cells may cause Cr levels to drop ( Verma *et al.*, 2016).

Hekmatnia et al. showed that different glioma grades can be identified using the signal intensities of NAA and Cr (Hekmatnia *et al.*, 2019). Our findings demonstrated that tumoral voxels have lower NAA levels than normal voxels (50382.85 $\pm$ 42832.33 and 97112.95 $\pm$ 57470.90) respectively. In malignant or benign tumors involving axonal loss, NAA, the second-most prevalent amino acid in the brain, is either significantly reduced or eliminated. The primary source of NAA signal loss in brain malignancies is, appropriately, the absence of the NAA synthesizing enzyme (aspartate N acetyltransferase) (Verma *et al*., 2016).

NAA is one of the most common amino acid derivatives in the brain and is a source of metabolic acetate in brain cells. NAA levels decreased in glioma tumors. It is believed that NAA hydrolysis produces the high quantities of acetate molecules required for lipogenesis in glioma tumor cells (Sathyanathan *et al.*, 2018).

The NAA has a significant function in glial signaling that is cell specific. They play a crucial role in brain function and development, the control of brain cell contacts, the upkeep of the nervous system, and even as a neurotransmitter in the central nervous system that functions as a partial agonist of N-methyl-d-aspartate receptors. The metabolism of glial cells depends on NAA.

Additionally, Canavan disease, a neurodegenerative disorder, has been linked to NAA aciduria (Baslow, 2017). A recent study made the case that brain stem cells, oligodendrocyte progenitor cells, and astrocytes might all act as the cell of origin for the development of glioblastoma (Chen *et al.*, 2019). Reduced NAA levels most likely have a metabolic and signaling effect that contributes to the development of glioblastoma.

Our findings demonstrated that the Pcho level was identical in tumoral and normal voxels. However, according to two separate investigations, Choline Kinase is overexpressed in several brain tumors, and a higher choline peak represents increased cell membrane synthesis, turnover, and integrity ( Verma *et al.*, 2016). According to Lu et al., choline levels must rise while NAA levels fall to assess the spatial extent of metabolic aberration and the ensuing tumor activity (Lu *et al.*, 2013).

Similar findings were reported in a different study, which demonstrated that while the NAA signal intensity reduced dramatically in the diaschisis cerebellar hemisphere, the choline and Cr signal intensities decreased only somewhat.

Higher levels of choline may be related to cell proliferation, whereas NAA is a measure of the density and survival of neurons). More research is necessary to determine the precise function of choline alterations in tumor metabolism.

Different glioblastoma biomarkers' lowered or raised ratios play a crucial role in diagnosis. In different research Pcho/NAA and Pcho/Cr ratios in recurrent glioma tumors were considerably greater than in radiation injury. However, compared to radiation damage, the NAA/Cr ratio was lower in recurrent glioma tumors (van Dijken *et al.*, 2017).

In addition, the Pcho/Cr and Pcho/NAA ratios in the radiation-damaged white matter were much higher than in the normal-appearing white matter, whereas the NAA/Cr ratio was lower in the radiation-damaged white matter. The largest significant Pcho/NAA ratio was found by Kazda et al. (Kazda *et al.*, 2016)

Sensitivity and specificity for glioblastoma recurrence (AUC=0.993; 100% sensitivity and 94.7% specificity). They also showed low sensitivity and specificity for the Pcho/Cr ratio (74.6 and 63.2%, respectively; AUC=0.691) (Kazda *et al.*, 2016). Contrarily, our results demonstrated that assessment of the Pcho/NAA ratio was the most effective technique for discriminating between normal and tumoral voxels. It showed a sensitivity and specificity of 83.3% and 28.8%, respectively, and an AUC of 0.836 at a cut-off of 0.7170.

In a comprehensive analysis, seven studies with a total of 261 high-grade glioma patients were examined. Analysis revealed that the combined sensitivity/specificity of the Pcho/NAA and Pcho/Cr ratios in peritumoral tissue were equivalent to 0.85/0.93 and 0.86/0.86, respectively. In the peritumoral area, the Pcho/NAA ratio had a larger AUC value and more specificity than the Pcho/ Cr ratio. They recommended using the Pcho/NAA ratio of the peritumoral area to improve MRS's ability to distinguish high-grade gliomas from metastases (Wang *et al.*, 2017). Our finding showed higher sensitivity and specificity of high-grade gliomas than metastases 83.3% /28.8% and 78.3% /37.5% respectively.

The correlation analysis offers insightful information on the connections between the most important items under investigation. Pcho and NAA have a highly significant positive correlation of 0.58. With a correlation value of 0.696 between Pcho/NAA and NAA, the two variables are strongly positively associated. The favorable outcome suggests that there is a strong correlation

between an increase in one variable's (Pcho/NAA) value and an increase in the other variable's (NAA) value. The positive correlation value can be interpreted as the majority of the study subjects had surgery to remove the tumor. As a result, both healthy and malignant membranes can be found where a tumor is located which can affect the correlation result.

Finally, by comparing GBM and other tumors, especially metastases, due to their comparable imaging features and contrast-enhanced patterns, glioblastomas and single brain metastases are sometimes difficult to distinguish with conventional MRI. surgical distinction before considering the potential differences in these cancers' surgical techniques and treatment procedures (Muccio *et al.*, 2019). Advanced MRI method, such as 1 H-MRS, is included in the standard clinical MRI practice and provide physiologic and metabolic data that may greatly aid in tumor distinction before surgery. By analyzing the intratumoral portion of the lesions, none of the evaluated MR methods and their associated characteristics were able to a certain degree to distinguish GBMs from metastatic tumors.

The metabolic ratios NAA/Cr, Pcho/Cr, and Pcho/NAA obtained from MRS corroborate the concept that the peritumoral area of glioblastomas is characterized by substantial infiltration of tumor cells whereas the peritumoral region of metastases includes nearly solely vasogenic edema.

By comparing GBM with Meningioma significant ratios are NAA/Cr and Pcho/NAA, our study showed higher NAA/Cr and lower Pcho/NAA in Meningioma 1.92 and 0.906 respectively, this is consistent with the fact that this disease does not contain cancerous cells.

By comparing GBM with Oligodendroglioma significant ratios are NAA/Cr and Pcho/NAA, our study showed lower NAA/Cr and higher Pcho/NAA in Oligodendroglioma 1.169 and 1.33

respectively, this is consistent with an increased probability of metabolic ratio of glia cells.

There was evidence of consistency between the test results and the biopsies' findings for each subject. This consensus was achieved after the radiologist carefully compared the verified GBM occurrences to the other potential illnesses under consideration. Surprisingly closely, the outcomes and the biopsy analysis agreed. This alignment highlights the precision of the diagnostic procedure. However, we cannot use MRS to substitute the biopsy-based diagnosis due to the limited sensitivity and specificity of the data. Nevertheless, we may use MRS as a backup diagnostic technique.

## 5.3 Conclusion

Advanced MRI method, such as 1 H-MRS, is included in the standard clinical MRI practice and provide physiologic and metabolic data that may greatly aid in tumor distinction before surgery. throughout the course of clinical practice to increase specificity and give an understanding of the underlying molecular characteristics of brain tumors.

However, due to the low sensitivity and specificity of the results, we cannot replace the diagnosis obtained through biopsy with MRS. Nevertheless, we can rely on MRS as a secondary diagnostic tool

The results of the current study showed that the most important and useful criteria for identifying tumoral and normal voxels in patients with glioblastoma who have 1HMRS are the NAA, Pcho/Cr, Cr/NAA, and Pcho/NAA ratios.

The most accurate diagnostic test was Pcho/NAA, with a sensitivity of 83.3% and a specificity of 28.8%. Cr/NAA was the second efficient test (sensitivity: 78.2%, specificity: 35.6%). The

Pcho/Crea Ratio was the third helpful test (sensitivity: 61.5%; specificity: 40.7%).

To find out whether 1H-MRS can distinguish between a brain tumor area and a healthy one, more research is required.

## 5.4. Recommendation

1. MRS Scan for Brain Tumors: Before considering surgical intervention, it is strongly advised that any patient exhibiting signs of a brain tumor undergo an MRS scan. This scan may help in making a precise diagnosis of the tumor that is already present, thus saving the patient from the hazards of needless surgery.

2. Implementation in MRI Departments: MRS scans have to be made available to all hospitals with MRI departments. If the required software is unavailable, hospitals might think about buying it. Hospitals can dramatically reduce the burden of surgical operations for patients with brain tumors by including MRS scans in their diagnostic regimens.

3. Radiology personnel should receive thorough training on conducting MRS scans properly and efficiently. Radiology technicians are responsible for operating MRI equipment. The advantages that MRS scans offer can be maximized by technicians by developing the relevant skills. Additionally, they should actively participate in talks with radiologists to jointly examine and interpret the scan data, improving the ability to diagnose brain cancers.

4. High-Field MRI Devices and Repetition: Replicating the study is advised to increase confidence in the use of MRS scans as a supporting tool for brain tumor diagnosis. High-field MRI machines like the 3 Tesla can be used to achieve this. Repeated studies and the use of cutting-edge MRI

technologies can help healthcare practitioners improve their diagnostic precision and delivery.

### 5.5. Strength of the Study

1. Specific Focus on Patients with GBM: This study's focus on patients with GBM, a condition known to have greater levels of metabolic indicators like Pcho and Cr in brain tumors, is a major strength. This focused strategy provided correct analysis and interpretation of the data as well as a thorough grasp of the features of the tumor.

2. Access to Specialized Software: The MRS scan was performed on the MRI machine at the Palestine Medical Complex thanks to the availability of specialized software. The accurate imaging and analysis of individuals with suspected brain tumors made possible by this program ensured accurate and thorough information for diagnosis and assessment.

3. Patient collaboration: The strength of the study was considerably increased by the high degree of patient collaboration and desire to engage in the research. These patients provided important information by giving their agreement to participate in the study, which increased the importance and dependability of the results overall. Their participation revealed a great dedication to advancing medical understanding and enhancing brain tumor diagnostic skills.

The focus on GBM patients, the availability of specialist software for MRS scans, and the willing involvement of the patients themselves are all factors that make this study strong. These elements add to the research's overall robustness and applicability in better comprehending and diagnosing brain cancers.

### 5.6. Study Limitations

1. Previous surgeries for tumor removal: The examination's capacity to determine the full existence

of the tumor was constrained by the inclusion of individuals who had already had tumor removal operations (2 patients new and 5 patients with tumor resection). Instead, attention was paid to studying tumor remains. As a result, there were fewer cancer cells found throughout the inspection, which might have affected the results and accuracy in general (the low sensitivity and specificity of the results).

2. MRI scanner Strength: To identify some of the metabolic parameters addressed in this work, a high-field MRI scanner with a stronger magnetic field is needed, such as the 3 Tesla. Because of this, many crucial metabolic parameters could not be discernible or properly evaluated using a typical 1.5 Tesla MRI machine, thus impacting the data's thoroughness.

3. A small number of GBM cases were included in the analysis. But the subjects were picked over nine months. For a more accurate evaluation of 1H-MRS power to identify GBM, larger-scale and larger-sample studies of the same sort may undoubtedly be helpful. The statistical power and generalizability of the results might be impacted by the small sample size of GBM patients.

4. Lack of Knowledge and Interest: Doctors have not been eager to submit any patients with tumors for examination since they are unfamiliar with using MR Spectroscopy to diagnose tumors. As a result, the study only included a few patients.

5. Tumor location and Fluid Presence: The presence of surrounding fluids and the position of the tumor may bring additional complexity and variables that might affect the examination's findings. When assessing the study's results, it is important to take into account how these variables may affect the precision and interpretation of the results.

6. This study faces challenges similar to traditional imaging procedures, including metallic substances in subjects' bodies, kidney issues, and titanium-based joint implants. Pre-MRS interventions may be necessary for kidney patients to restore physiological parameters before the examination, requiring solutions and medications.

### 5.7. Future work

1. Replicating the Study with a High-Field MRI Device: Replicating the study using a high-field MRI machine, such as the 3 Tesla, is one possible direction for future research. This may offer improved imaging capabilities and maybe produce more precise and thorough data. By adopting cutting-edge technology, researchers may look at how well MRS scans work for detecting brain tumors and perhaps learn more about their characteristics.

2. Investigating MRS Scans for Other Types of Cancer: Research on the efficiency of MRS scans in identifying cancers in other body regions, such as breast tumors and prostate cancer, is an interesting field for future investigation. Researchers may evaluate the diagnostic utility of MRS scans in various clinical settings by looking at the metabolic markers unique to certain kinds of malignancies. This could aid in the creation of more thorough, non-invasive diagnostic methods for diverse tumor types.

3. Comparative Studies: Research on MRS scans and other diagnostic methods might benefit from comparative studies. Researchers may better grasp the benefits and drawbacks of MRS in a variety of clinical settings by contrasting the precision, sensitivity, and specificity of MRS scans with well-established techniques like biopsy or other imaging modalities. This can improve how MRS scans are used for tumor diagnosis and treatment planning and help decision-makers make more educated choices.

4. Multi-Center Trials and Bigger Sample Sizes: Future research may take into account performing multi-center trials with a bigger sample size to further confirm the results and guarantee their generalizability. As a result, there may be more support for the efficacy of MRS scans in the diagnosis of brain tumors or other types of cancers. This may boost the statistical power and robustness of the study. Collaboration across various medical facilities can increase the validity and significance of the study findings.

5. Longitudinal Studies and Follow-Up: Studies that track patients over a lengthy period might offer insightful information about the development and response of malignancies to therapy. MRS scans can be used in long-term follow-up regimens to help researchers track metabolic changes in tumors and assess the effectiveness of therapies. This can help in creating individualized treatment plans and enhancing patient results.

Overall, these new avenues can increase our knowledge of MRS scans' diagnostic capability and their suitability for various tumor forms. Researchers can advance medical knowledge, improve diagnostic procedures, and enhance patient care by focusing on these topics.

## References


Arcalis, N. *et al.* (2011) 'Patterns of contrast enhancement in the brain and meninges. A Pictorial Review.', in. European Congress of Radiology-ECR 2011.

Baik, J. *et al.* (2016) 'Primary Pontine Glioblastoma Multiforme: A Case Report and Review of the Literature', *Journal of the Korean Society of Radiology*, 75, pp. 121–125.

Baslow, M. H. (2017) 'Rescuing Canavan disease: engineering the wrong cell at the right time', *Journal of Inherited Metabolic Disease*, 40, pp. 627–628.

Bertholdo, D., Watcharakorn, A. and Castillo, M. (2013) 'Brain proton magnetic resonance spectroscopy: introduction and overview', *Neuroimaging Clinics*, 23, pp. 359–380.

Bhaskaran, M. *et al.* (2020) 'Current perspectives on therapies, including drug delivery systems, for managing glioblastoma multiforme', *ACS chemical neuroscience*, 11, pp. 2962–2977.

Chen, H. *et al.* (2019) 'Overexpression of miR-1283 inhibits cell proliferation and invasion of glioma cells by targeting ATF4', *Oncology Research*, 27, p. 325.

Ciurleo, R. *et al.* (2014) 'Magnetic resonance spectroscopy: an in vivo molecular imaging biomarker for Parkinson's disease?', *BioMed Research International*, 2014.

Crain, I. D. *et al.* (2017) 'Improving the utility of 1H-MRS for the differentiation of glioma recurrence from radiation necrosis', *Journal of Neuro-Oncology*, 133, pp.97–105. doi: 10.1007/s11060-017-2407-y.

D'Alessio, A. *et al.* (2019) 'Pathological and molecular features of glioblastoma and its peritumoral tissue', *Cancers*, 11, pp. 2. doi: 10.3390/cancers11040469.

Deviers, A. *et al.* (2014) 'Evaluation of the lactate-to-N-acetyl-aspartate ratio defined with magnetic resonance spectroscopic imaging before radiation therapy as a new predictive marker of the site of relapse in patients with glioblastoma multiforme', *International Journal of Radiation Oncology* Biology* Physics*, 90, pp. 385–393.

Dezfouli, M. A. P. *et al.* (2017) 'Quantification of 1H–MRS signals based on sparse metabolite profiles in the time–frequency domain', *NMR in Biomedicine*, 30, pp.1.

Diego De Stefani, Maria Patron, and R. R. (2015) '乳鼠心肌提取 HHS Public Access', *Physiology & behavior*, 176, pp. 139–148. doi: 10.1016/j.ijrobp.2014.03.049.Volumetric.

van Dijken, B. R. J. *et al.* (2017) 'Diagnostic accuracy of magnetic resonance imaging techniques for treatment response evaluation in patients with high-grade glioma, a systematic review and meta-analysis', *European radiology*, 27, pp. 4129–4144.

Donahoe (2012) '基因的改变NIH Public Access', *Molecular and Cellular Biochemistry*, 23, pp. 1–7. doi: 10.1016/j.nic.2010.04.003.Imaging.

Duong, T. Q. (2012) 'Chapter 24 MRI in Experimental Stroke', 8, pp. 473–485. doi: 10.1007/978-

1-61737-992-5.

Einstein, D. B. *et al.* (2012) 'Phase II trial of radiosurgery to magnetic resonance spectroscopy–defined high-risk tumor volumes in patients with glioblastoma multiforme', *International Journal of Radiation Oncology* Biology* Physics*, 84, pp. 668–674.

Ekici, S. *et al.* (2020) 'Characterization of dysregulated glutamine metabolism in human glioma tissue with 1H NMR', *Scientific Reports*, 10, pp. 1–10. doi: 10.1038/s41598-020-76982-7.

Gharzeddine, K. *et al.* (2019) 'MR perfusion and MR spectroscopy of brain neoplasms', *Radiologic Clinics*, 57, pp. 1177–1188.

Green, R. A. *et al.* (2012) 'The theory and practice of hyperpolarization in magnetic resonance using parahydrogen', *Progress in nuclear magnetic resonance spectroscopy*, 67, pp. 1–48.

Haider, H. M., Zakarya, S. and Abu-Hegazy, M. (2012) 'White matter microstructure and cognitive dysfunction in systemic lupus patients', *Egyptian Journal of Neurology, Psychiatry and Neurosurgery*, 49, pp. 199–206.

Hangel, G. *et al.* (2022) 'Emerging methods and applications of ultra-high field MR spectroscopic imaging in the human brain', *Analytical Biochemistry*, 638, pp. 114479. doi: 10.1016/j.ab.2021.114479.

Hanif, F. *et al.* (2017) 'Glioblastoma multiforme: A review of its epidemiology and pathogenesis through clinical presentation and treatment', *Asian Pacific Journal of Cancer Prevention*, 18, pp. 3–9. doi: 10.22034/APJCP.2017.18.1.3.

Hassan, Q. *et al.* (2019) 'Improvements in lipid suppression for 1 H NMR-based metabolomics: Applications to solution-state and HR-MAS NMR in natural and in vivo samples', *Magnetic Resonance in Chemistry*, 57, pp. 69–81. doi: 10.1002/mrc.4814.

Hauser, K. and Matthes, J. (2017) 'Medical students' medication communication skills regarding drug prescription—a qualitative analysis of simulated physician-patient consultations', *European Journal of Clinical Pharmacology*, 73, pp. 429–435. doi: 10.1007/s00228-016-2192-0.

Hekmatnia, A. *et al.* (2019) 'Diagnostic value of Magnetic Resonance Spectroscopy (MRS) for detection of Brain Tumors in patients', *Med. Sci*, 23, pp. 939–945.

Kalra, S. (2019) 'Magnetic resonance spectroscopy in ALS', *Frontiers in Neurology*, 10, pp. 1–7. doi: 10.3389/fneur.2019.00482.

Kazda, T. *et al.* (2016) 'Advanced MRI increases the diagnostic accuracy of recurrent glioblastoma: Single institution thresholds and validation of MR spectroscopy and diffusion weighted MR imaging', *NeuroImage: Clinical*, 11, pp. 316–321.

Kim, T.-M. *et al.* (2015) 'Subclonal Genomic Architectures of Primary and Metastatic Colorectal Cancer Based on Intratumoral Genetic HeterogeneityITH of Colorectal Cancers with Metastases', *Clinical Cancer Research*, 21, pp. 4461–4472.

Kohler, I. *et al.* (2017) 'Integrating clinical metabolomics-based biomarker discovery and clinical

pharmacology to enable precision medicine', *European journal of pharmaceutical sciences*, 109, pp. S15–S21.

Lu, D., Sun, Y. and Wan, S. (2013) 'Brain tumor classification using non-negative and local non-negative matrix factorization', in *2013 IEEE International Conference on Signal Processing, Communication and Computing (ICSPCC 2013)*. 80, pp. 1–4.

Ma, R. *et al.* (2013) 'Diagnostic and prognostic markers in gliomas–an update', *British journal of neurosurgery*, 27, pp. 311–315.

Manoranjan, B. and Provias, J. P. (2011) 'Congenital brain tumors: diagnostic pitfalls and therapeutic interventions', *Journal of Child Neurology*, 26, pp. 599–614.

Mansoory, M. S. *et al.* (2020) 'Analysis of glioblastoma multiforme tumor metabolites using multivoxel magnetic resonance spectroscopy', *Avicenna Journal of Medical Biotechnology*, 12, pp. 107–115.

Moffett, J. R. *et al.* (2014) 'N-Acetylaspartate and N-acetylaspartylglutamate in central nervous system health and disease', in *Magnetic Resonance Spectroscopy*. pp. 71–90.

Muccio, C. F. *et al.* (2019) 'Solitary cerebral metastases vs. high-grade gliomas: usefulness of two MRI signs in the differential diagnosis', *Anticancer Research*, 39, pp. 4905–4909.

Mukherjee, D. *et al.* (2014) 'Effectiveness of radiotherapy for elderly patients with anaplastic gliomas', *Journal of Clinical Neuroscience*, 21, pp. 773–778. doi: 10.1016/j.jocn.2013.09.004.

Nayak, L., Lee, E. Q. and Wen, P. Y. (2012) 'Epidemiology of brain metastases', *Current oncology reports*, 14, pp. 48–54.

Network, N. (2014) 'SCIENTIFIC',.(Statistical Simulation of MR Spectroscopy of Brain Lesions by Neural Network), *The Internet Journal of Radiology*, 17 , pp. 1.

Nishihara, R. *et al.* (2015) 'Molecular pathological epidemiology gives clues to paradoxical findings', *European journal of epidemiology*, 30, pp. 1129–1135.

Ohgaki, H. and Kleihues, P. (2013) 'The Definition of Primary and Secondary GlioblastomaDefinition of Primary and Secondary Glioblastomas', *Clinical cancer research*, 19, pp. 764–772.

Ohka, F., Natsume, A. and Wakabayashi, T. (2012) 'Current trends in targeted therapies for glioblastoma multiforme', *Neurology Research International*, 2012. doi: 10.1155/2012/878425.

Opoku-Darko, M., Amuah, J. E. and Kelly, J. J. P. (2018) 'Surgical resection of anterior and posterior butterfly glioblastoma', *World neurosurgery*, 110, pp. e612–e620.

Pacheva, I. *et al.* (2016) 'Creatine Deficiency Syndrome could be Missed Easily: A Case Report of Guanidinoacetate Methyltransferase Deficiency Presented with Neurodevelopmental Delay, Seizures, and Behavioral Changes, but Normal Structural MRI.', *Annals of clinical and laboratory science*, 46, pp. 557–61. Available at: http://www.ncbi.nlm.nih.gov/pubmed/27650626.

Parra, N. A. *et al.* (2014) 'Volumetric spectroscopic imaging of glioblastoma multiforme radiation treatment volumes', *International Journal of Radiation Oncology* Biology* Physics*, 90, pp. 376–384.

Rahimian, E. *et al.* (2013) 'Proton MR spectroscopy in the diagnostic evaluation of suspected mitochondrial disease in Iran', *Iranian Journal of Child Neurology*, 7, pp. 12.

Romano, A. *et al.* (2022) 'Single brain metastasis versus glioblastoma multiforme: a VOI-based multiparametric analysis for differential diagnosis', *Radiologia Medica*, 127, pp. 490–497. doi: 10.1007/s11547-022-01480-x.

Rosso, I. M. *et al.* (2017) 'Hippocampus Glutamate and N-Acetyl Aspartate Markers of Excitotoxic Neuronal Compromise in Posttraumatic Stress Disorder', *Neuropsychopharmacology*, 42, pp. 1698–1705. doi: 10.1038/npp.2017.32.

Ru, P. *et al.* (2013) 'Tumor Metabolism of Malignant Gliomas', *Cancers*, 5, pp. 1469–1484. doi: 10.3390/cancers5041469.

Sanli, A. *et al.* (2010) 'Unusual manifestations of primary Glioblastoma Multiforme: A report of three cases', *Surgical Neurology International*, 1, pp. 87. doi: 10.4103/2152-7806.74146.

Sathyanathan, B. P. *et al.* (2018) '3T proton MR spectroscopy evaluation of spinal cord lesions', *Indian Journal of Radiology and Imaging*, 28, pp. 285–295.

Taylor, O. G., Brzozowski, J. S. and Skelding, K. A. (2019) 'Glioblastoma multiforme: An overview of emerging therapeutic targets', *Frontiers in Oncology*, 9, pp. 1–11. doi: 10.3389/fonc.2019.00963.

Tome-Garcia, J. *et al.* (2017) 'Prospective Isolation and Comparison of Human Germinal Matrix and Glioblastoma EGFR+ Populations with Stem Cell Properties', *Stem Cell Reports*, 8, pp. 1421–1429. doi: 10.1016/j.stemcr.2017.03.019.

Tsougos, I. *et al.* (2012) 'Differentiation of glioblastoma multiforme from metastatic brain tumor using proton magnetic resonance spectroscopy, diffusion and perfusion metrics at 3 T', *Cancer imaging*, 12, pp. 423.

Urbanska, K. *et al.* (2014) 'Glioblastoma multiforme - An overview', *Wspolczesna Onkologia*, 18, pp. 307–312. doi: 10.5114/wo.2014.40559.

Verma, A *et al.* (2016) 'Magnetic resonance spectroscopy-revisiting the biochemical and molecular milieu of brain tumors. BBA clinical ,5,pp. 170–178'.

Verma, Ashish *et al.* (2016) 'Magnetic resonance spectroscopy—revisiting the biochemical and molecular milieu of brain tumors', *BBA clinical*, 5, pp. 170–178.

Wang, Q. *et al.* (2017) 'Role of magnetic resonance spectroscopy to differentiate high-grade gliomas from metastases', *Tumor Biology*, 39,pp.3. doi: 10.1177/1010428317710030.

Weinberg, B. D. *et al.* (2021) 'Clinical Applications of Magnetic Resonance Spectroscopy in Brain Tumors: From Diagnosis to Treatment', *Radiologic Clinics of North America*, 59, pp. 349–362.

doi: 10.1016/j.rcl.2021.01.004.

Xu, Y. Y. *et al.* (2015) 'Development of targeted therapies in treatment of glioblastoma', *Cancer Biology and Medicine*, 12, pp. 223–237. doi: 10.7497/j.issn.2095-3941.2015.0020.

Yan, J. L. *et al.* (2019) 'Multimodal MRI characteristics of the glioblastoma infiltration beyond contrast enhancement', *Therapeutic Advances in Neurological Disorders*, 12, pp. 1–10. doi: 10.1177/1756286419844664.

Zhen, L. *et al.* (2010) 'Multiple extracranial metastases from secondary glioblastoma multiforme: a case report and review of the literature', *Journal of neuro-oncology*, 97, pp. 451–457.

# Appendices

## Appendix A: MOH Approval

State of Palestine
Ministry of Health
Assistant Deputy for Allied Medical
Professions and Blood Banks

دولة فلسطين
وزارة الصحـــــــة
الوكيل المساعد
للمهن الطبية المساندة وبنوك الدم

الاخ الدكتور معتصم محيسن المحتـــــــــرم
الوكيل المساعد لشؤون المستشفيات والطوارئ

2023-517
10/4/2023

الموضوع: تسهيل مهمة

تحية طيبة وبعد,,,

بعد التحية وبالاشارة للموضوع أعلاه، يرجى تسهيل مهمة الطالب ياسر محمد ابراهيم منصور ماجستير في برنامج التصوير المقطعي والتصوير بالرنين المغناطيسي من جامعة العربية الامريكية لعمل مشروع بحث بعنوان

(MR spectrocscopy MRS and MR spectroscopic imaging MRSI for the non-invasive evaluation of glioblastoma multiform GBM tumor)

تحت اشراف الدكتور عبدالناصر عاصي وذلك لحصوله على المعلومات اللازمة للدراسة في مجمع فلسطين الطبي ، على ان يتم التعامل مع كافة المعلومات بسرية تامة وتستخدم لأغراض البحث العلمي فقط.

تفضلوا بقبول فائق الاحترام,,,

أخوكم
أسامة النجار
الوكيل المساعد
للمهن الطبية المساندة وبنوك

Lana

Ministry of Health – Ramallah
Ministry of Health - Nablus

TelFax: 022964402: تلفاكس
e-mail :parmed@moh.ps
TelFax: 09-2335821: تلفاكس

وزارة الصحة –رام الله
وزارة الصحة – نابلس

## Appendix B: Information Sheet

Arab American University
Scientific Research Deanship
Ethical Review Committee

الجامعـــة العربيـــة الأمريكيـــة
عمادة البحث العلمي
لجنة اخلاقيات البحث العلمي

**ورقة معلومات المشاركين**

**AAUP-IRB Code No.:** …… 2023/A/29/N……..
**AAUP-IRB Date:** ……1 4 February 2023……

**عنوان البحث: التصوير الطيفي بالرنين المغناطيسي للتقيم غير الجراحي لاورام ارومي الدبقي المتعدد**

……

نود أن ندعوكم للمشاركة في دراسة بحثية. قبل أن تقرر ما إذا كنت تود المشاركة، عليك أن تفهم سبب إجراء البحث وما الذي سيتضمنه. يرجى تخصيص بعض الوقت لقراءة المعلومات التالية بعناية؛ أخبر آخرين عن الدراسة إذا كنت ترغب في ذلك.
اسألنا عما إذا كان هناك أي شيء غير واضح أو ما إذا كنت ترغب مزيد من المعلومات. خذ وقتًا لأخذ قرار ما إذا كنت ترغب في المشاركة أم لا.

---

١. ما هو الغرض من هذه الدراسة ؟

اثبات ان فحص التصوير الطيفي بالرنين المغناطيسي قادر على تشخيص ورم ارومي الدبقي المتعدد بدون الحاجة الى اجراء عملية جراحية

……

٢. لماذا هذه الدراسة مهمة ؟

تكمن اهمية هذه الدراسة في تجنيب المريض من الخضوع لعملية جراحية لاخذ خزعة من الورم واختصار الفترة الزمنية التي ينتظرها المريض لاظهار نتيجة العينة مما يؤدي الى تاخير البداية بالعلاج

……

٣. ما هو الإجراء الذي يتم اختباره ؟ (إذا كان منطبقا)

الاجراء المطلوب هو فقط الخضوع لاجراء صورة رنين مغناطيسي اضافية مع فحص الرنين المغناطيسي العادية هي صورة التصوير الطيفي بالرنين المغناطيسي ومدتها عشرة دقائق

……

٤. لماذا دُعيت للمشاركة في هذه الدراسة ؟

لان المرض الذي تعاني منه هو الذي تقوم عليه الدراسة

……

٥. من يجب ألا يشارك في الدراسة ؟

لايوجد اي مانع لاي مريض من عمل الصورة لانها لا تؤدي الى اي ضرر لكن يستثنى من المشاركة المرضى الذين يعانون من فشل كلوي وايضا المرضى الذين خضعو لعمليات زراعة مفصل او جهاز منظم قلب

جنين - ص.ب: ٢٤٠ هاتف: ٩٧٠-٤-٢٤١٨٨٨٨ فاكس: ٩٧٠-٤-٢٥١٠٨١٣
Jenin - P.O. Box: 240 Tel: 970-4-2418888 Fax: 970-4-2510813 E-mail: src@aaup.edu Website: www.aaup.edu

٦. هل يمكنني رفض المشاركة في الدراسة ؟

نعم يمكن لاي شخص ان يرفض المشاركة

.....

٧. ماذا سيحدث لي إذا شاركت ؟

لا يوجد اي ضرر من عمل صورة الرنين المغناطيسي

.....

٨. إلى متى سأشارك في هذه الدراسة ؟

مدة هذه الدراسة خمسة الى ستة شهور

.....

٩. ما هي المخاطر المحتملة ؟

لا يوجد مخاطر لهذه الدراسة

.....

١٠. ما هي الفوائد المحتملة؟

هذه الدراسة مفيدة مستقبلا للمرضى الذين يظهر عليهم اعراض هذا المرض حيث انهم لن يخضعوا لاجراء عملية جراحية وسيتم البدء بالعلاج معهم بفترة زمنية قليلة

.....

١١. من سيتمكن من الوصول إلى سجلاتي الطبية وبيانات البحث ؟

لن يتم الدخول الى سجلاتك الطبية فقط صورة الرنين المغناطيسي سيتم تحليل بياناتها وادراجها بالدراسة

.....

١٢. هل ستبقى سجلاتي/بياناتي سرية ؟

نعم ستبقى السجلات سرية حيث ان صورة الرنين سيتم اخذها بدون اسم

.....

١٣. ماذا سيحدث لأي عينات أعطيها ؟ إذا كان منطبقا

لا يوجد اخذ عينات

.....

١٤. ماذا سيحدث إذا لم أرغب في الاستمرار في الدراسة ؟

يمكن للمشارك بالدراسة الانسحاب من المشاركة باي وقت

.....

١٥. ماذا سيحدث لنتائج الدراسة البحثية ؟
سيتم تعميم الدراسة على وزارة الصحة لاعتمادها ومن ثم تطبيق اجراء الفحص من قبل مراكز تصوير الرنين المغناطيسي

.....

١٦. هل سأحصل على تعويض عن المشاركة في هذه الدراسة ؟
لا يوجد اي تعويض مادي

.....

١٧. من الذي يجب أن أتصل به إذا كانت لدي أسئلة/مشاكل أثناء الدراسة ؟

**تفاصيل الاتصال بالباحث:**

الطالب ياسر محمد ابراهيم منصور جوال رقم ٠٥٩٨٩١٩٨٩١

.....

١٨. من الذي يجب أن أتصل به إذا كنت غير راضٍ عن كيفية إجراء الدراسة ؟

مشرف الدراسة الدكتور عبد الناصر عاصي جوال رقم ٠٥٩٨١١١٢٧٩

.....

Ethical Review Committee
Deanship of Scientific Research
Arab American University-Palestine (AAUP)
Email: src@aaup.edu

## Appendix C: IRB Approval

Arab American University- Palestine
Deanship of Scientific Research
IRB committee
Tel: 04-241-8888, ext 1196
E-mail: irb.aaup@aaup.edu

الجامعة العربية الامريكية- فلسطين
عمادة البحث العلمي
لجنة أخلاقيات البحث العلمي
تلفون: 04-241-8888 1196 ext
البريد الالكتروني: irb.aaup@aaup.edu

# IRB Approval Letter

**Study Title:** MR spectroscopy (MRS) and MR spectroscopic imaging (MRSI) for the non-invasive evaluation of glioblastoma multiform (GBM) tumors.

**Submitted by:** Yasser Mohammad Ibrahim Mansour

**Date received:** 09th January 2023

**Date reviewed:** 10th February 2023

**Date approved:** 14th February 2023

Your Study titled **"MR spectroscopy (MRS) and MR spectroscopic imaging (MRSI) for the non-invasive evaluation of glioblastoma multiform (GBM) tumors"** With archived number **2023/A/29/N** was reviewed by the Arab American University IRB committee and was approved on 14th February 2023

**Reham Khalaf-Nazzal, MD, PhD**
**IRB committee chairman**
**Arab American University of Palestine**

**General Conditions:**
1. Valid for 1 year from date of approval.
2. It is important to inform the committee with any modification of the approved study protocol.
3. The committee appreciates a copy of the research when accomplished.

لجنة أخلاقيات البحث العلمي في الجامعة العربية الامريكية

IRB at Arab American University

## Appendix D: AAUP Approval

Arab American University
Faculty of Graduate Studies

الجامعة العربية الأمريكية
كلية الدراسات العليا

2023/3/9

السّادة وزارة الصحة الفلسطينية المحترمين.

تسهيل مهمة بحثية

تحية طيبة وبعد،

تهديكم كلية الدراسات العليا في الجامعة العربية الأمريكية أطيب التحيات، وبالإشارة الى الموضوع أعلاه، تشهد كلية الدراسات العليا في الجامعة أن الطالب **ياسر محمد إبراهيم منصور** والذي يحمل الرقم الجامعي**202113120**هو طالب ماجستير في برنامج التصوير المقطعي والتصوير بالرنين المغناطيسي ويعمل على رسالة الماجستير الخاصة به بعنوان:

" MR spectroscopy (MRS) and MR spectroscopic imaging (MRSI) for the non-invasive evaluation of glioblastoma multiform (GBM) tumor تحت اشراف الدكتور عبد الناصر عاصي" نأمل من حضرتكم الإيعاز لمن يلزم لمساعدته للحصول على المعلومات اللازمة للدراسة، علماً أن المعلومات ستستخدم لغاية البحث فقط وسيتم التعامل معها بغاية السرية، وقد أعطيت هذه الرسالة بناءً على طلبه.

وتفضلوا بقبول فائق الاحترام

عميد كلية الدراسات العليا

د. نوار قطب

كلية الدراسات العليا
FACULTY OF GRADUATE STUDIES



Jenin Tel: +970-4-2418888 Ext.:1471,1472 Fax: +970-4-2510810 P.O. Box:240
Ramallah Tel: +970-2-2941999 Fax: +970-2-2941979 Abu Qash - Near Alrehan
E-mail: FGS@aaup.edu ; PGS@aaup.edu Website: www.aaup.edu

# الملخص


## مقدمة

الورم الأرومي الدبقي متعدد الأشكال (GBM) ، هو الورم الأكثر شيوعًا وتكرارًا في الجهاز العصبي المركزي بين السكان البالغين ، والذي يشكل 40٪ من جميع أنواع أورام المخ و 15٪ إلى 20٪ من الأورام عالية الدرجة. تعتبر GBM مشكلة صحية عامة حرجة ، فهي ورم نادر مع حدوث عالمي أقل من 10 لكل 100،000 شخص ومعدل البقاء على قيد الحياة 14-15 شهرًا بعد التشخيص. في جميع الفئات العمرية ، تمثل 50٪ من جميع الأورام الدبقية.

تُستخدم طريقة تصوير غير جراحية تسمى التحليل الطيفي بالرنين المغناطيسي (MRS) لفحص التغيرات الأيضية في أورام الدماغ الخبيثة. في العمل الحالي ، تم استخدام MRS multivoxel للتحقيق في المستقلبات المهمة في أورام GBM. منذ تقريره الأول في الثمانينيات ، تقدم التحليل الطيفي بالرنين المغناطيسي (MRS)للدماغ البشري بسرعة. اكتسبت Proton MRS شعبية في التسعينيات بسبب حساسيتها المتزايدة وراحتها الأكبر نتيجة لتطوير تقنيات محسنة للتوطين المكاني وقمع المياه (حيث يمكن إجراؤها دون تعديل الأجهزة في معظم أجهزة التصوير بالرنين المغناطيسي ، على عكس MRS من النوى الأخرى . (يتم إجراء الفحص باستخدام ماسح التصوير بالرنين المغناطيسي).

## الغرض من الدراسة

الغرض من هذه الدراسة هو تقييم وتشخيص الورم الأرومي الدبقي متعدد الأشكال (GBM) باستخدام طريقة تصوير غير جراحية تسمى التحليل الطيفي بالرنين المغناطيسي (MRS) لإنقاذ المريض من الاضطرار إلى الخضوع لجراحة الخزعة. وتجنيب المريض المخاطر المصاحبة له.

## طرق الدراسة

كانت الدراسة عبارة عن دراسة كمية مقطعية وتدخلية لتقييم الورم الأرومي الدبقي متعدد الأشكال باستخدام التحليل الطيفي بالرنين المغناطيسي وفعالية MRS للاستغناء عن الخزعة في ممارسة عمل قسم التصوير بالرنين المغناطيسي في المستشفيات الحكومية الفلسطينية ، وخاصة في مجمع فلسطين الطبي وخاصة في قسم الرنين المغناطيسي.

في هذه الدراسة ، تم جمع المعلومات من 7 أفراد تم تشخيص إصابتهم GBMوبراءة اختراع واحدة مع الانبثاث وبراءة اختراع واحدة مع ورم سحائي وبراءة اختراع واحدة مع ورم الدبقيات قليلة التغصُّن من أغسطس 2022 إلى يونيو 2023. باستخدام GE multivoxel MRS مع مجال مغناطيسي شدة 1.5 تم الحصول على البيانات بواسطة بروتوكول Point-Resolved Spectroscopy (PRESS) مع TE

144 =مللي ثانية و TR = 1570 مللي ثانية. تم استخراج وتقييم نسبة Pcho و NAA و Cr و Pcho Cr /ونسبة Pcho / NAA و NAA / Cho ونسبة NAA / Cr ومستقلبات Cr / NAA وتقييمها إحصائيًا.

## نتيجة

بالنسبة لإجمالي عدد وحدات البكسل لـ GBM ، سواء كانت طبيعية أو ورمية ، كان مستوى قيم نسبة التمثيل الغذائي لـ NAA / Cr و NAA / Cho و Cho / Cr و Cho / NAA و Cho تركيز (1.2 ، 0.90 ، 1.81 ، 1.91) ، 66999.17) على التوالي لفوكسل الورم و (2.34 ، 1.67 ، 1.49 ، 0. 69 ، 62585.15) على التوالي بالنسبة للفوكسل الطبيعي ، كانت نسبة فوكسل الورم أعلى بكثير من النسبة الطبيعية ، وتركيز تشو أعلى من المعدل الطبيعي فوكسل.

## خاتمة

**في** الختام ، أظهرت نتائج الدراسة الحالية أن نسب NAA و Pcho / Cr و Cr / NAA و / Pcho NAAهي المعايير الأكثر أهمية وعملية للتمييز بين الفوكسل الورمي والطبيعي في المرضى الذين يعانون من الورم الأرومي الدبقي الذين لديهم HMRS.1 كان Pcho / NAA أعلى قيمة تشخيصية (حساسية 83.3 ٪ و 28.8 ٪ ٪ خصوصية). الاختبار الثاني الفعال كان Cr / NAA (الحساسية: 78.2٪ ، النوعية: 35.6٪). الاختبار الثالث المفيد كان) Pcho / Crea Ratio الحساسية:( 61.5٪ ، النوعية: 40.7٪) ومع ذلك , نظرا لانخفاض حساسية وخصوصية النتائج لا يمكننا استبدال التشخيص الذي يتم الحصول عليه من خلال الخزعة بالتصوير الطيفي بالرنين المغناطيسي , وع ذلك يمكننا الاعتماد عليه كتشخيص ثانوي .